Performance Evaluation and Enhancement for AF Two-Way Relaying in the Presence of Channel Estimation Error

by

Chenyuan Wang
B.Sc., Beijing University of Posts and Telecommunications, 2009

A Dissertation Submitted in Partial Fulfillment of the
Requirements for the Degree of

MASTER OF APPLIED SCIENCE

in the Department of Electrical and Computer Engineering

Performance Evaluation and Enhancement for AF Two-Way Relaying in the Presence of Channel Estimation Error

by

Chenyuan Wang
B.Sc., Beijing University of Posts and Telecommunications, 2009

Supervisory Committee

Dr. Xiaodai Dong, Supervisor
(Department of Electrical and Computer Engineering)

Dr. T. Aaron Gulliver, Departmental Member
(Department of Electrical and Computer Engineering)

Supervisory Committee

Dr. Xiaodai Dong, Supervisor
(Department of Electrical and Computer Engineering)

Dr. T. Aaron Gulliver, Departmental Member
(Department of Electrical and Computer Engineering)

ABSTRACT

Cooperative relaying is a promising diversity achieving technique to provide reliable transmission, high throughput and extensive coverage for wireless networks in a variety of applications. Two-way relaying is a spectrally efficient protocol, providing one solution to overcome the half-duplex loss in one-way relay channels. Moreover, incorporating the multiple-input-multiple-output (MIMO) technology can further improve the spectral efficiency and diversity gain. A lot of related work has been performed on the two-way relay network (TWRN), but most of them assume perfect channel state information (CSI). In a realistic scenario, however, the channel is estimated and the estimation error exists. So in this thesis, we explicitly take into account the CSI error, and investigate its impact on the performance of amplify-and-forward (AF) TWRN where either multiple distributed single-antenna relays or a single multiple-antenna relay station is exploited.

For the distributed relay network, we consider imperfect self-interference cancellation at both sources that exchange information with the help of multiple relays, and maximal ratio combining (MRC) is then applied to improve the decision statistics under imperfect signal detection. The system performance degradation in terms of outage probability and average bit-error rate (BER) are analyzed, as well as their asymptotic trend. To further improve the spectral efficiency while maintain the spatial diversity, we utilize the maximum minimum (*Max-Min*) relay selection (RS), and examine the impact of imperfect CSI on this single RS scheme. To mitigate the negative effect of imperfect CSI, we resort to adaptive power allocation (PA) by minimizing either the outage probability or the average BER, which can be cast as a

Geometric Programming (GP) problem. Numerical results verify the correctness of our analysis and show that the adaptive PA scheme outperforms the equal PA scheme under the aggregated effect of imperfect CSI.

When employing a single MIMO relay, the problem of robust MIMO relay design has been dealt with by considering the fact that only imperfect CSI is available. We design the MIMO relay based upon the CSI estimates, where the estimation errors are included to attain the robust design under the worst-case philosophy. The optimization problem corresponding to the robust MIMO relay design is shown to be nonconvex. This motivates the pursuit of semidefinite relaxation (SDR) coupled with the randomization technique to obtain computationally efficient high-quality approximate solutions. Numerical simulations compare the proposed MIMO relay with the existing nonrobust method, and therefore validate its robustness against the channel uncertainty.

Contents

List of Tables

List of Figures

List of Abbreviations

AF	amplify-and-forward
ANC	analogy network coding
AWGN	additive white Gaussian noise
BER	bit-error rate
c.d.f.	cumulative density function
CGRV	complex Gaussian random variable
CSI	channel state information
DF	decode-and-forward
GP	Geometric Programming
i.i.d.	independent and identically distributed
LP	linear programming
Max-Min	maximum minimum
MGF	moment generating function
MIMO	multiple-input-multiple-output
MRC	maximal ratio combining
MSE	mean-square error
OWRN	one-way relay network
p.d.f.	probability density function
PA	power allocation
QoS	quality of service
QPSK	quadrature phase shifted keying
r.v.	random variable
RS	relay selection
SDP	semidefinite programming
SDR	semidefinite relaxation
SNR	signal-to-noise ratio
SOC	second-order cone

TDD	time division duplexing
TWRN	two-way relay network

ACKNOWLEDGEMENTS

First and foremost, I owe my deepest gratitude to my supervisor Dr. Xiaodai Dong. Her sage advice, insightful comments, and patient encouragement aided the writing of this thesis. I am also grateful for her continuous support to my M.A.Sc study, and her personal guidance leading me to taste the pleasure of research and publication.

Besides, I would like to show my gratitude to my committee member Dr. T. Aaron Gulliver for his insightful guidance and constructive comments, and to Dr. Jianping Pan for being as the external examiner.

I would like to thank my graduate course instructors, Dr. Wu-Sheng Lu, Dr. Lin Cai, Dr. Antoniou, Dr. Kui Wu, for their good teaching, great efforts to explain things clearly and simply, kind assistance with projects, and so on. Especially Dr. Wu-Sheng Lu providing me sound suggestion and help to my research deserves special mention. I wish to thank in addition Dr. Alfonso Gracia-Saz from Department of Mathematics and Statistics for his assistance with solving my mathematical problem in my research.

I wish to thank my best friend Ping Li, for her accompanying and helping me to get through my tough times in Victoria. Her persistent consolation, emotional support, and pure-hearted caring provide me the courage to face and overcome the difficulties. Ping indeed feels like a family.

I am indebted to my many student colleagues for providing a stimulating and fun environment in which to learn and grow. I am especially grateful to Ted C.-K. Liu, Yang Song, Moyuan Chen, Teng Ge, Congzhi Liu, Xi Tu, Dan Li, Jie Yan, Li Ji, and Xuan Wang.

Lastly, and most importantly, I wish to thank my parents, Yusheng Wang and Qiuhua Ma. They bore me, raised me, supported me, taught me, and loved me. To them I dedicate this thesis.

DEDICATION

To my dearest parents

Chapter 1

Introduction

Relay networks have gained a lot of interest recently for the benefit of spectral efficiency [1–6]. Comparing to one-way half-duplex relaying, bidirectional relaying is a spectrally efficient protocol to simultaneously communicate between two users [4, 5]. The two widely used relaying protocols in one-way relaying – amplify-and-forward (AF) and decode-and-forward (DF) [2, 3] – are naturally inherited by the two-way relaying. Attracted by the benefits of lower complexity and easier implementation, AF protocol is more desirable for practical consideration if compared to DF.

Typically, AF two-way relaying consists of two sources transmitting information simultaneously to the relay in the first phase, and the relay amplifying the received signals and broadcasting in the second phase. The process of linear amplifying the sum signal received from both sources and then retransmitting the resulting signal is also referred to as analogy network coding (ANC). The essential of ANC relies on the observation that the collision at the relay in the first phase is totally harmless, and that the so-called self-interference can be removed from the received signals at the sources before data detection since both sources know their own transmitted signals. The ANC has been extensively employed in the AF two-way relay network (TWRN) [6–12].

1.1 Motivation and Related Work

In practice, channel state information (CSI) must be estimated, and therefore estimation error exists. So it is important to study the influence of channel estimation error on the system performance in AF TWRN. Furthermore, the strategies to enhance the

performance and combat the channel uncertainty resulting from the estimation error are also of practical interest. In this section, the related work in the literature for AF ANC-based TWRN has been investigated, which demonstrates the lack of research in the area of performance analysis and enhancement with imperfect CSI, and motivates the work of this thesis.

1.1.1 Two-Way Distributed Relay Network

In the presence of multiple single-antenna relays, channel estimation for TWRN has been comprehensively studied [6, 13]. In [13], the training sequences from two source nodes are designed to minimize the mean-square error (MSE) of channel estimation according to zero forcing criterion. Gao, *et. al.* in [6] propose two channel estimators for the AF TWRN – the maximum-likelihood estimator and the linear maximum signal to noise ratio estimator. In these papers, the impact of inaccurate channel estimation is measured by how well the estimator can approximate the actual channels in the MSE sense.

Another line of research has been focused on power allocation (PA) for TWRN [9, 10]. In [9], a PA scheme taking into account the trade-off of outage probability between the two terminals for a single relay TWRN is presented. Adaptive PA algorithms are proposed in [10] to maximize the instantaneous sum rate and minimize the system outage probability for multi-relay systems. In the presence of multiple relays, single relay selection (RS) is exploited in [10] to further improve the system performance. Similar to one-way relay network (OWRN), performing RS in TWRN is attractive due to its superior rate performance and cost effectiveness in implementation. Several RS schemes in an AF TWRN with the two-step transmission procedure are studied in [11], including best-relay selection, best-worse-channel selection, and maximum-harmonic-mean selection. All these RS schemes can achieve the full diversity order. Researchers in [12] propose a simple suboptimal min-max criterion for RS where a single relay that minimizes the maximum symbol error rate between the two sources is selected. Although most papers consider PA and RS to improve the system performance, they often assume perfect self-interference cancellation under perfect CSI condition.

It's not difficult to find that the existing work on imperfect CSI all consider OWRN [14–16]; while those for TWRN only take into account the design of channel estimators. To the best of our knowledge, performance analysis of TWRN and further

enhancement by PA with imperfect CSI have not yet been studied.

1.1.2 Two-Way MIMO Relay Network

Since multiple-input-multiple-output (MIMO) systems are able to support high-data rates by combating fading and interference, it is reasonable to exploit the advantages of MIMO systems by accommodating multiple antennas at the relay node. Hence, by introducing MIMO relay to assist the single-antenna sources communicating with each other, the system can achieve impressive spectral efficiency improvements and provide significant throughput gains.

The optimization of the AF MIMO relay precoder is extensively studied in [17–19]. In [17], the ANC-based two-way relay channel is considered and the optimal structure for MIMO relay to achieve the capacity region is presented. Li, *et. al.* in [18] extend to the relaying scheme that is suitable for any configurations of relays or antennas, and design the relay precoder to minimize the MSE between the received and transmitted signals with sum power constraints on all relays. In [19], the sources are equipped with multiple antennas instead of a single antenna, so by using the minimum MSE receivers the joint optimization of both the source and relay precoders with respect to either minimal weighted sum-MSE or maximum weighted sum-rate of bidirectional links is investigated. All optimal precoder design methods mentioned above assume perfect self-interference cancellation under perfect CSI condition.

In practice, CSI needs to be estimated at the receiver by using a training sequence and fed back to the transmitter. In time division duplexing (TDD) systems, the reverse-link estimation is possible at the transmitter by exploiting the channel reciprocity [20]. Therefore, the error always exists in CSI due to various sources of imperfection, such as estimation Gaussian noise, quantization errors, and interference through the feedback channel. The optimal designs based upon the perfect CSI are extremely sensitive to channel errors, which results in system performance degrading. In fact, developing optimal designs that are robust to channel uncertainty is not a new topic in one-way relaying, and can be found in the literature [21–23]. Chalise, *et. al.* in [21] provide a robust design of MIMO relay precoder taking into account the channel uncertainty for a system with multiple source-destination pairs assisted by a single MIMO relay station, and further extend this work to multiple multi-antenna relays in [22]. In [23], the same system as in [21] is considered, and the MIMO relay precoder as well as the destination filters are jointly designed to provide robustness

to errors in CSI, and both stochastic error model and norm-bounded error model are investigated.

In the literature, the robust design in the presence of imperfect CSI in two-way MIMO relay network is still a complete blank, but its research significance mandates a thorough and timely study.

1.2 Contributions

The main contributions of this thesis are summarized as follows.

First of all, the two-way distributed relay network consisting of a pair of communicating sources and multiple single-antenna relays is considered. Under imperfect channel condition, the system performance of outage probability and average bit-error rate (BER) are analyzed. It's worth to note that we take into account both the imperfect self-interference cancelation and imperfect data detection due to the CSI estimation error. Furthermore, instead of employing all relays, we also examine the impact of imperfect CSI on a single RS scheme. To mitigate the negative impact of imperfect CSI, we show that PA by minimizing either the outage probability or the BER can be suitably casted as the Geometric Programming (GP) problem.

Secondly, we exploit a single MIMO relay station to substitute the multiple single-antenna relays in the aforementioned AF TWRN, and investigate the problem of designing the MIMO relay precoder by taking into account the imperfect CSI. We design the MIMO relay based upon the CSI estimates, where the estimation errors are included to attain the robust design under the worst-case philosophy. In particular, the worst-case transmission power at the MIMO relay is minimized while guaranteeing the worst-case quality of service (QoS) requirements that the received signal-to-noise ratio (SNR) at both sources are above a prescribed threshold value. The optimization problem turns out nonconvex, and we resort to the semidefinite relaxation (SDR) coupled with the randomization technique to obtain computationally efficient high-quality approximate solutions.

1.3 Thesis Outline

The rest of this thesis is organized as follows:

Chapter 2 analyzes the system outage probability and average BER of the AF dis-

tributed TWRN in the presence of CSI estimation errors, as well as their asymptotic performance. Thereafter, the maximum minimum (*Max-Min*) single RS scheme is presented to improve the rate performance. Finally, the adaptive PA is proposed to further mitigate the effect of imperfect CSI on system performance.

Chapter 3 considers the two-way MIMO relay network, and designs the AF MIMO relay that provides robustness to the channel uncertainty resulting from the estimation error by using the worst-case approach. Designing the robust MIMO relay turns out to be a nonconvex optimization problem. This chapter shows that the original optimization problem can be reformulated and then relaxed to a convex problem that can be solved using interior point methods. Then the randomization loop is carried out to obtain an approximate solution to the original problem.

Chapter 4 concludes the thesis and suggests possible future work.

Chapter 2

Impact of Channel Estimation Error on the Performance of AF Two-Way Distributed Relaying

In this chapter, we consider an AF ANC-based TWRN with a pair of communicating sources and multiple relays under the influence of CSI estimation error. The CSI estimation error is modeled as the actual channel plus a complex Gaussian random variable (CGRV) as in [15, 16]. The source is assumed to have obtained an estimate of its own channel so that it can perform the self-interference cancellation prior to maximal ratio combining (MRC) from all relays to improve its decision statistics. We take into account both the imperfect self-interference cancellation and the imperfect data detection due to CSI estimation error. We first derive the effective end-to-end SNR after self-interference cancellation and MRC. From this, we then derive both the outage probability and system BER, as well as their asymptotic expressions. Furthermore, we examine the impact of imperfect CSI on RS. To mitigate the negative impact of imperfect CSI, we also show that PA by minimizing either the outage probability or the average BER can be suitably cast as a GP [24–26] problem which can be solved by efficient convex programming technique [27]. Numerical results show the correctness of the derived expressions, and demonstrate that the adaptive PA outperforms the equal PA scheme.

The remainder of the chapter is organized as follows. Section (Sec.) 2.1 introduces the system model under consideration. Sec. 2.2 derives the effective SNRs under CSI estimation error, and together with both the outage probability and the BER

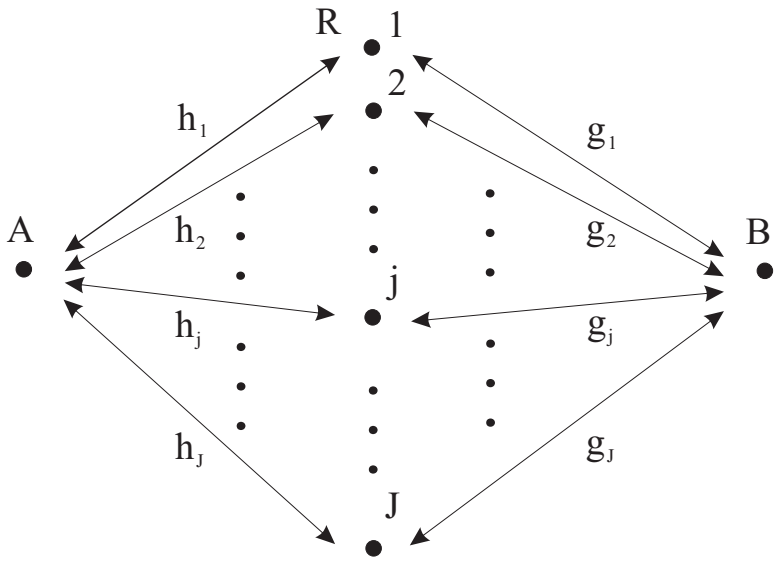

Figure 2.1: System model for AF two-way distributed relay network.

expressions. RS with imperfect CSI is studied in Sec. 2.3, and the corresponding outage probability and average BER performance when considering estimation error are determined. In Sec. 2.4, adaptive PA scheme is formulated as a GP problem to improve the performance under imperfect CSI. Numerical results are given in Sec. 2.5, and Sec. 2.6 concludes this chapter.

2.1 System Model

We consider a two-way AF relay-assisted system consisting of two sources A and B, and J relays $R_1, R_2, \ldots, R_J$. As shown in Fig. 2.1, there is no direct link between A and B, and they exchange information with the help of J relays. We assume that the TWRN operates under TDD mode, which means both the uplink and downlink channels occupy the same frequency slot, but are differentiated in a time duplex manner in information exchange. In the system herein, we consider a two-phase cooperative strategy where the first phase involves the pair of sources broadcasting to all of the relays. The second phase is where each individual relay retransmits, in an orthogonal manner, its scaled information to the sources. During Phase I, both sources A and B broadcast their information simultaneously in the first time slot, which is also referred to as ANC in the literature [6, 9–12]. The signals received at

the relays are

$$r_i = \sqrt{P_A} h_i x_A + \sqrt{P_B} g_i x_B + n_{r_i}, \quad i = 1, 2, \ldots J, \tag{2.1}$$

where x_A and x_B denote the transmitted signals with unit average energy, i.e., $E[|x_A|^2] = 1$ and $E[|x_B|^2] = 1$, and P_A, P_B are the transmission powers of A and B. Variables h_i and g_i are discrete baseband equivalent channel coefficients for both sides of the link to the ith relay, as indicated in Fig. 2.1. The channel coefficients h_i, g_i are modeled as CGRVs with zero-mean and variances $\sigma_{h_i}^2$ and $\sigma_{g_i}^2$, respectively, i.e., $h_i \sim \mathcal{CN}(0, \sigma_{h_i}^2)$, $g_i \sim \mathcal{CN}(0, \sigma_{g_i}^2)$. Parameter n_{r_i} is circularly symmetric additive white Gaussian noise (AWGN) with variance N_{r_i}, i.e., $n_{r_i} \sim \mathcal{CN}(0, N_{r_i})$.

In Phase II, all relays simply amplify the received signals and retransmit to either source. Let the estimates of channel coefficients for both links to the ith relay be $\hat{h}_i$ and $\hat{g}_i$. We assume that both pairs h_i, $\hat{h}_i$ and g_i, $\hat{g}_i$ can be modeled as jointly ergodic and stationary Gaussian processes. The relations between the actual channels and the estimated channels are given by

$$h_i = \hat{h}_i + e_{h_i}, \text{ and } g_i = \hat{g}_i + e_{g_i}, \tag{2.2}$$

where e_{h_i} and e_{g_i} are the channel estimation errors following the distribution of $\mathcal{CN}(0, \sigma_{e_{h_i}}^2)$ and $\mathcal{CN}(0, \sigma_{e_{g_i}}^2)$, respectively. Note that e_{h_i} and $\hat{h}_i$ are independent if $\hat{h}_i$ is the minimum mean square error estimation of h_i. In this thesis, we consider independent e_{h_i} and $\hat{h}_i$ and independent e_{g_i} and $\hat{g}_i$. Therefore, $\hat{h}_i$ and $\hat{g}_i$ are distributed as $\mathcal{CN}(0, \sigma_{h_i}^2 - \sigma_{e_{h_i}}^2)$ and $\mathcal{CN}(0, \sigma_{g_i}^2 - \sigma_{e_{g_i}}^2)$. Note that $\sigma_{e_{h_i}}^2$ and $\sigma_{e_{g_i}}^2$ are parameters that indicate the quality of the channel estimation schemes.

Now, for the ith ($i = 1, 2, \ldots J$) relay in Phase II, it scales its received signal by a factor β_i and retransmits in the $(i+1)$th time slot. We exploit the instantaneous power scaling factor β_i [2,3,9,10,15,16] that is chosen to scale the transmission power at the ith relay to unity, i.e.,

$$\beta_i = \sqrt{\frac{P_{r_i}}{P_A(|\hat{h}_i|^2 + \sigma_{e_{h_i}}^2) + P_B(|\hat{g}_i|^2 + \sigma_{e_{g_i}}^2) + N_{r_i}}}, \tag{2.3}$$

where P_{r_i} is the transmission power of the ith relay. Because β_i varies depending on the instantaneous CSI, the relay using β_i defined in (2.3) is called variable gain relay.

The signals received by the two sources from the ith relay are

$$\begin{aligned} y_{A,i} &= \sqrt{P_A} h_i^2 \beta_i x_A + \sqrt{P_B} h_i g_i \beta_i x_B + h_i \beta_i n_{r_i} + n_{A,i}, \\ y_{B,i} &= \sqrt{P_B} g_i^2 \beta_i x_B + \sqrt{P_A} h_i g_i \beta_i x_A + g_i \beta_i n_{r_i} + n_{B,i}, \end{aligned} \tag{2.4}$$

where $n_{A,i}$ and $n_{B,i}$ denote the AWGN of the relay-source channels with variance $N_{A,i}$ and $N_{B,i}$, respectively. Then the self-interference can be cancelled as $z_{A,i} = y_{A,i} - \sqrt{P_A}\hat{h}_i^2 \beta_i x_A$ and $z_{B,i} = y_{B,i} - \sqrt{P_B}\hat{g}_i^2 \beta_i x_B$. The self-interference cannot be completely removed due to imperfect CSI even if the sources know their own transmitted data. To this end, we consider the case where the cancellation of self-interference will lead to some new interference terms.

Note that each relay needs the CSI h_i and g_i to form the instantaneous power scaling factor, and each source needs the corresponding link CSI h_i and g_i to remove self-interference and perform the subsequent combining and detection. In this chapter, we assume the CSI estimates used at the relay and the sources are identical, which can be realized as follows. Each link CSI is estimated once at the relay by employing pilots at the sources, e.g., estimators from [6,13]. The relay then forwards the channel estimates to both sources. The manners as to how CSI is estimated and how it can be forwarded are beyond the scope of this thesis.

2.2 Performance Analysis on Impact of CSI Estimation Error

In this section, we will first determine the effective total SNRs at the sources. Based on the effective SNRs, we then derive both the outage probability and average BER under the impact of CSI estimation error. We validate our derivation with simulation results in Sec. 2.5.

2.2.1 End-to-End SNR for Relay Links with Estimation Error

The received signals after self-interference cancellation at two sources can be expressed as

$$\begin{aligned} z_{A,i} &= \sqrt{P_B} h_i g_i \beta_i x_B + \underbrace{h_i \beta_i n_{r_i} + n_{A,i} + \sqrt{P_A} h_i^2 \beta_i x_A - \sqrt{P_A} \hat{h}_i^2 \beta_i x_A}_{n_{A,i}^{tot}}, \\ z_{B,i} &= \sqrt{P_A} h_i g_i \beta_i x_A + \underbrace{g_i \beta_i n_{r_i} + n_{B,i} + \sqrt{P_B} g_i^2 \beta_i x_B - \sqrt{P_B} \hat{g}_i^2 \beta_i x_B}_{n_{B,i}^{tot}}, \end{aligned} \tag{2.5}$$

for $i = 1, 2, \ldots J$, where $n_{k,i}^{tot}$ ($k \in \{A, B\}$) is defined as the total noise on the ith relay branch at source k with power $N_{k,i}^{tot}$ given in (2.7).

At the source k, MRC is performed to improve the decision statistics by jointly combining the received signals $z_{k,i}$ from all relays after self-interference cancellation. By multiplying the MRC weight $w_{k,i}$, the combiner output at k can be written as

$$Z_k = \sum_{i=1}^{J} Z_{k,i} = \sum_{i=1}^{J} w_{k,i} z_{k,i}, \tag{2.6}$$

where

$$\begin{aligned} w_{A,i} &= \frac{\sqrt{P_B} \hat{h}_i^* \hat{g}_i^* \beta_i}{N_{A,i}^{tot}}, \text{ and } w_{B,i} = \frac{\sqrt{P_A} \hat{h}_i^* \hat{g}_i^* \beta_i}{N_{B,i}^{tot}}, \\ N_{A,i}^{tot} &= |\hat{h}_i|^2 \beta_i^2 N_{r_i} + N_{A,i} + 4P_A |\hat{h}_i|^2 \sigma_{e_{h_i}}^2 \beta_i^2 + 2P_A \sigma_{e_{h_i}}^4 \beta_i^2, \\ N_{B,i}^{tot} &= |\hat{g}_i|^2 \beta_i^2 N_{r_i} + N_{B,i} + 4P_B |\hat{g}_i|^2 \sigma_{e_{g_i}}^2 \beta_i^2 + 2P_B \sigma_{e_{g_i}}^4 \beta_i^2. \end{aligned} \tag{2.7}$$

We first consider the transmission from B to A. By replacing (2.2) in $Z_{A,i}$, the MRC output of the ith relay link in terms of the estimated channel coefficients $\hat{h}_i$, $\hat{g}_i$, and the estimation errors e_{h_i}, e_{g_i}, is given by

$$Z_{A,i} = w_{A,i} \left[\sqrt{P_B} (\hat{h}_i + e_{h_i})(\hat{g}_i + e_{g_i}) \beta_i x_B + (\hat{h}_i + e_{h_i}) \beta_i n_{r_i} + n_{A,i} + \sqrt{P_A} (2\hat{h}_i e_{h_i} + e_{h_i}^2) \beta_i x_A \right], \tag{2.8}$$

where β_i, $w_{A,i}$, $N_{A,i}^{tot}$ are given by (2.3) and (2.7), respectively. The last term in (2.8) results from the imperfect self-interference cancellation due to channel estimation error.

Then, (2.8) can be divided into the signal, the channel estimation error and noise parts, which are given respectively as,

$$s_{A,i} = \frac{P_B \beta_i^2 |\hat{h}_i|^2 |\hat{g}_i|^2}{N_{A,i}^{tot}} x_B, \tag{2.9}$$

$$\epsilon_{A,i} = \frac{P_B \beta_i^2 \hat{h}_i^* \hat{g}_i^*}{N_{A,i}^{tot}} (\hat{h}_i e_{g_i} + \hat{g}_i e_{h_i} + e_{h_i} e_{g_i}) x_B + \frac{\sqrt{P_A}\sqrt{P_B}\beta_i^2 \hat{h}_i^* \hat{g}_i^*}{N_{A,i}^{tot}} (2\hat{h}_i e_{h_i} + e_{h_i}^2) x_A, \tag{2.10}$$

$$\eta_{A,i} = \frac{\sqrt{P_B}\beta_i \hat{h}_i^* \hat{g}_i^*}{N_{A,i}^{tot}} (\beta_i \hat{h}_i n_{r_i} + \beta_i e_{h_i} n_{r_i} + n_{A,i}). \tag{2.11}$$

Using the property of mutual independence among $\hat{h}_i$, $\hat{g}_i$, e_{h_i}, e_{g_i}, n_{r_i} and $n_{A,i}$ [15,16], we can obtain the variance of the sum of (2.10) and (2.11). Thus, the effective SNR for the ith relay link can be derived as

$$\gamma_{A,i}^{\text{eff}} = \frac{P_B P_{r_i} |\hat{h}_i|^2 |\hat{g}_i|^2}{P_B |\hat{g}_i|^2 (P_{r_i} \sigma_{e_{h_i}}^2 + N_{A,i}) + P_{r_i} |\hat{h}_i|^2 (P_B \sigma_{e_{g_i}}^2 + N_{r_i}) + P_A |\hat{h}_i|^2 N_{A,i} + 4 P_A P_{r_i} |\hat{h}_i|^2 \sigma_{e_{h_i}}^2 + \kappa_i}, \tag{2.12}$$

where $\kappa_i = P_B P_{r_i} \sigma_{e_{h_i}}^2 \sigma_{e_{g_i}}^2 + 2 P_A P_{r_i} \sigma_{e_{h_i}}^4 + P_{r_i} \sigma_{e_{h_i}}^2 N_{r_i} + P_A \sigma_{e_{h_i}}^2 N_{A,i} + P_B \sigma_{e_{g_i}}^2 N_{A,i} + N_{A,i} N_{r_i}$. It should be noted that both (2.10) and (2.11) comprise of two Gaussian random variables (r.v.'s) multiplying together, which would result in total noise not being Gaussian. However, the result of this multiplication will not have a drastic effect on performance since it is of small value in practice where both estimation error and noise variances are small[1].

The form of (2.12) is not easily tractable. However, assuming both estimation error and noise variances are relatively small in practical system operating range, e.g., by transmitting a large number of pilots at medium to high SNR[2], the last four terms of κ_i can be ignored. Similarly, the first and second terms can also be ignored since they are the product of two estimation error variances. Hence, κ_i approaches a very small number at high SNR, and can be negligible compared to other terms in

[1] Low estimation error and noise variances can be realized by transmitting a number of pilots at medium to high SNR.

[2] The variance of estimation error can be modeled as a deceasing function of both SNR and the length of training sequences K, that is, $\sigma_e^2 = \frac{1}{K \cdot \text{SNR}}$ [28]. So the impact of the last four terms of κ_i on (2.12) is insignificant if $K > 10$.

the denominator[3]. Therefore, (2.12) can be simplified to

$$\gamma_{A,i}^{\text{eff}} \simeq \frac{\hat{\gamma}_{1,i}\ \hat{\gamma}_{2,i}}{\hat{\gamma}_{1,i}\left(1+\frac{P_{r_i}\sigma_{e_{h_i}}^2}{N_{A,i}}\right)+\hat{\gamma}_{2,i}\left(1+\frac{P_B\sigma_{e_{g_i}}^2}{N_{r_i}}\right)+\hat{\gamma}_{3,i}\left(1+\frac{4P_{r_i}\sigma_{e_{h_i}}^2}{N_{A,i}}\right)}, \tag{2.13}$$

where $\hat{\gamma}_{1,i} := \frac{P_B|\hat{g}_i|^2}{N_{r_i}}$ and $\hat{\gamma}_{2,i} := \frac{P_{r_i}|\hat{h}_i|^2}{N_{A,i}}$ are the estimated SNRs for the link from B to R_i and from R_i to A, respectively; and $\hat{\gamma}_{3,i} := \frac{P_A|\hat{h}_i|^2}{N_{r_i}}$ is the estimated SNR for the link from A to R_i. We also define $\hat{\gamma}_{4,i} := \frac{P_{r_i}|\hat{g}_i|^2}{N_{B,i}}$ as the estimated SNR of the link from R_i to B.

By observing the definition of $\hat{\gamma}_{2,i}$ and $\hat{\gamma}_{3,i}$, we obtain the relationship of them as

$$\hat{\gamma}_{3,i} = \hat{\gamma}_{2,i}\frac{P_A}{P_{r_i}}\frac{N_{A,i}}{N_{r_i}}. \tag{2.14}$$

Using (2.14) to subsitute $\hat{\gamma}_{2,i}$ for $\hat{\gamma}_{3,i}$, (2.13) can be further simplified in the form of the harmonic mean as

$$\gamma_{A,i}^{\text{eff}} \simeq \frac{\gamma_{1,i}^{\text{eff}}\gamma_{2,i}^{\text{eff}}}{\gamma_{1,i}^{\text{eff}}+\gamma_{2,i}^{\text{eff}}}, \tag{2.15}$$

where

$$\gamma_{1,i}^{\text{eff}} := \frac{\hat{\gamma}_{1,i}}{\left(1+\frac{P_B\sigma_{e_{g_i}}^2}{N_{r_i}}+\frac{P_A}{P_{r_i}}\frac{N_{A,i}}{N_{r_i}}+\frac{4P_A\sigma_{e_{h_i}}^2}{N_{r_i}}\right)}, \text{ and } \gamma_{2,i}^{\text{eff}} := \frac{\hat{\gamma}_{2,i}}{\left(1+\frac{P_{r_i}\sigma_{e_{h_i}}^2}{N_{A,i}}\right)}. \tag{2.16}$$

It can be easily seen that the instantaneous effective SNRs $\gamma_{1,i}^{\text{eff}}$ and $\gamma_{2,i}^{\text{eff}}$ are independent and exponentially distributed with mean respectively as

$$\begin{aligned} E[\gamma_{1,i}^{\text{eff}}] := \bar{\gamma}_{1,i}^{\text{eff}} &= \frac{P_B(\sigma_{g_i}^2-\sigma_{e_{g_i}}^2)}{P_B\sigma_{e_{g_i}}^2+\frac{P_A}{P_{r_i}}N_{A,i}+4P_A\sigma_{e_{h_i}}^2+N_{r_i}}, \\ E[\gamma_{2,i}^{\text{eff}}] := \bar{\gamma}_{2,i}^{\text{eff}} &= \frac{P_{r_i}(\sigma_{h_i}^2-\sigma_{e_{h_i}}^2)}{P_{r_i}\sigma_{e_{h_i}}^2+N_{A,i}}. \end{aligned} \tag{2.17}$$

Similarly, we can derive the effective SNR of the ith relay branch at source B for

[3]Through Monte Carlo simulations, the MSE between (2.12) and (2.13) is close to zero under all SNR range at $\sigma_{e_{h_i}}^2 = \sigma_{e_{g_i}}^2 \leq 0.01$. Therefore, this approximation can be safely used for practical purposes.

data transmission from A as

$$\gamma_{B,i}^{\text{eff}} = \frac{\hat{\gamma}_{3,i}\ \hat{\gamma}_{4,i}}{\hat{\gamma}_{3,i}\left(1+\frac{P_{r_i}\sigma_{e_{g_i}}^2}{N_{B,i}}\right)+\hat{\gamma}_{4,i}\left(1+\frac{P_A\sigma_{e_{h_i}}^2}{N_{r_i}}+\frac{P_B}{P_{r_i}}\frac{N_{B,i}}{N_{r_i}}+\frac{4P_B\sigma_{e_{g_i}}^2}{N_{r_i}}\right)}. \tag{2.18}$$

For the MRC in (2.6) at the source, the effective combiner output SNR is then the sum of effective SNRs on each relay branch. Thus, the total effective SNRs at both sources can be written mathematically as

$$\gamma_A^{\text{eff}} = \sum_{i=1}^{J}\gamma_{A,i}^{\text{eff}},\ \text{and}\ \gamma_B^{\text{eff}} = \sum_{i=1}^{J}\gamma_{B,i}^{\text{eff}}. \tag{2.19}$$

2.2.2 Outage Probability Analysis

In the AF TWRN, an outage of any two sources will cause an overall outage. We denote the probability that the instantaneous capacity falls below certain rate for the source k ($k \in \{A, B\}$) as $\Pr\{C_k < R_k\}$, where C_k and R_k are the instantaneous rate and the target transmission rate for k, respectively. Then we can write the overall outage probability of the AF TWRN as

$$P_{out} = \Pr\{C_A < R_A\} + \Pr\{C_B < R_B\} - \Pr\{C_A < R_A, C_B < R_B\} \tag{2.20}$$

$$\simeq \Pr\{C_A < R_A\} + \Pr\{C_B < R_B\} - \Pr\{C_A < R_A\}\Pr\{C_B < R_B\}. \tag{2.21}$$

where

$$\Pr\{C_k < R_k\} = \Pr\left\{\frac{1}{(J+1)}\log_2\left(1+\sum_{i=1}^{J}\gamma_{k,i}^{\text{eff}}\right) < R_k\right\} = \Pr\left\{\sum_{i=1}^{J}\gamma_{k,i}^{\text{eff}} < \gamma_{th,k}\right\} \tag{2.22}$$

is the outage probability at source k denoted by P_{out}^k, $\gamma_{th,k} = 2^{(J+1)R_k} - 1$ is the outage threshold, and the factor $1/(J+1)$ is due to the two-phase transmission in $(J+1)$ time slots. Considering the dependency between C_A and C_B [29], a tight upper bound can be derived for $\Pr\{C_A < R_A, C_B < R_B\}$ by using a similar approach to [29] for the single relay case. For the multiple relay case, the derivation of $\Pr\{C_A < R_A, C_B < R_B\}$ is not tractable due to the sum term $\sum_{i=1}^{J}\gamma_{k,i}^{\text{eff}}$ in (2.22). However, (2.21) can

be used to approximate the system outage probability[4]. Moreover, the last term in (2.20) and (2.21) can be ignored in the asymptotically high SNR region.

Due to the symmetry of the end-to-end SNRs at two sources, we determine the closed-form expression of $\Pr\{C_A < R_A\}$, and similar approach can be applied to obtain $\Pr\{C_B < R_B\}$. In order to find the outage probability, we need to derive the probability density function (p.d.f.) or cumulative density function (c.d.f.) of variable $\gamma_A^{\text{eff}} = \sum_{i=1}^{J} \gamma_{A,i}^{\text{eff}}$. Since $\gamma_{A,i}^{\text{eff}}$ is the harmonic mean of two exponential r.v.'s given in (2.16), let $X_{1,i} = \gamma_{1,i}^{\text{eff}}$ and $X_{2,i} = \gamma_{2,i}^{\text{eff}}$ be two independent exponential r.v.'s with parameters $\beta_{1,i} = 1/\bar{\gamma}_{1,i}^{\text{eff}}$ and $\beta_{2,i} = 1/\bar{\gamma}_{2,i}^{\text{eff}}$. By using [30, Theorem 1], the c.d.f. of $\gamma_{A,i}^{\text{eff}}$ is given by

$$\Pr\{\gamma_{A,i}^{\text{eff}} < s\} = 1 - 2s\sqrt{\beta_{1,i}\beta_{2,i}}e^{-s(\beta_{1,i}+\beta_{2,i})}K_1\left(2s\sqrt{\beta_{1,i}\beta_{2,i}}\right), \tag{2.23}$$

where $K_1(\cdot)$ is the first order modified Bessel function of the second kind [31]. The function $K_1(\cdot)$ can be approximated as $K_1(x) \simeq 1/x$ for small x [31]. Therefore, at high SNR, we can approximate $\gamma_{A,i}^{\text{eff}}$ as an exponential r.v. with rate $\lambda_{A,i} = 1/\bar{\gamma}_{1,i}^{\text{eff}} + 1/\bar{\gamma}_{2,i}^{\text{eff}}$. The c.d.f. of $\gamma_{A,i}^{\text{eff}}$ is then $P_{\gamma_{A,i}^{\text{eff}}}(s) = \Pr\{\gamma_{A,i}^{\text{eff}} < s\} = 1 - e^{-\lambda_{A,i}s}$.

Now, γ_A^{eff} becomes the sum of J independent exponential r.v.'s $\gamma_{A,i}^{\text{eff}}$. Assuming the $\lambda_{A,i}$'s to be distinct, the c.d.f. of γ_A^{eff} can be obtained to be [32]

$$\Pr\{\gamma_A^{\text{eff}} < s\} \simeq \sum_{i=1}^{J}\left(\prod_{m=1,m\neq i}^{J}\frac{\lambda_{A,m}}{\lambda_{A,m}-\lambda_{A,i}}\right)(1-e^{-\lambda_{A,i}s}). \tag{2.24}$$

If the $\lambda_{A,i}$ is the same, denoted by λ_A, then γ_A^{eff} follows Gamma distribution with scale $1/\lambda_A$ and shape factor J, i.e., $\gamma_A^{\text{eff}} \sim \Gamma(J, 1/\lambda_A)$, where $\Gamma(a,b)$ is the Gamma distribution with shape factor a and scale b. Note that both distinct and identical $\lambda_{A,i}$ cases are special cases of the general form where some of $\lambda_{A,i}$'s are the same and others are different. These two cases are in fact portraying two extreme network topologies in cooperative communications[5] which can encompass the two extreme ends of performance under imperfect CSI with all other different $\lambda_{A,i}$ combinations falling in between. The general case is not included here, but it is straightforward

[4]Through Monte Carlo simulations, the difference between (2.20) and (2.21) is shown to be small in the whole SNR range for the multiple relay case, so the approximation in (2.21) has negligible effect on the performance.

[5]The first case where $\lambda_{A,i}$'s are different can be an example of where mobiles are used as relays whereas the second case in which $\lambda_{A,i}$'s are identical can be an example of where a fixed relay station with closely grouped antennas is used to relay information.

to extend our analysis to include the general form. For the interested readers, the p.d.f. of γ_A^{eff} with some distinct and some identical $\lambda_{A,i}$'s can be found in [33].

Furthermore, in fading channels, the error performance is dominated by the probability of having deep fades, which in turn pertains to the behavior of the p.d.f. of the effective SNR at A, $p_{\gamma_A^{\text{eff}}}(s)$, around zero. Therefore, by differentiating (2.24) and using Taylor series to expand $p_{\gamma_A^{\text{eff}}}(s)$, the p.d.f. of γ_A^{eff} can be written in the form of $\sum_{n=0}^{J-1} p_{\gamma_A^{\text{eff}}}^{(n)}(0)s^n/n! + o(s^J)$, the expansion of $p_{\gamma_A^{\text{eff}}}(s)$ at the origin[6]. That is

$$p_{\gamma_A^{\text{eff}}}(s) = \sum_{n=0}^{J-1} \left(\sum_{i=1}^{J} \left(\prod_{m=1, m\neq i}^{J} \frac{\lambda_{A,m}}{\lambda_{A,m} - \lambda_{A,i}} \right) \lambda_{A,i}^{n+1} \right) \frac{(-1)^n}{(n)!} s^n + o(s^J). \tag{2.25}$$

Since the r.v. γ_A^{eff} is the sum of J r.v.'s of $\gamma_{A,i}^{\text{eff}}$, which is the harmonic mean of $\gamma_{1,i}^{\text{eff}}$ and $\gamma_{2,i}^{\text{eff}}$, it can be shown that the derivatives of $p_{\gamma_A^{\text{eff}}}(s)$ evaluated at zero up to order $(J-2)$ are zero, while the $(J-1)^{th}$ order derivative is given by $\prod_{i=1}^{J} \left(p_{\gamma_{1,i}^{\text{eff}}}(0) + p_{\gamma_{2,i}^{\text{eff}}}(0) \right)$ [34, Proposition 1, 2]. So we have the coefficients of s^n to be zero for $n \in [1, J-2]$, and the coefficient of s^{J-1} to be $\prod_{i=1}^{J} \left(1/\bar{\gamma}_{1,i}^{\text{eff}} + 1/\bar{\gamma}_{2,i}^{\text{eff}} \right)$. Then by integrating $p_{\gamma_A^{\text{eff}}}(s)$, the asymptotic outage probability at A can now be expressed as

$$P_{out}^{A}(\gamma_{th,A}) = \Pr\{\gamma_A^{\text{eff}} < \gamma_{th,A}\} \simeq \frac{1}{J!} \cdot \prod_{i=1}^{J} \left(\frac{1}{\bar{\gamma}_{1,i}^{\text{eff}}} + \frac{1}{\bar{\gamma}_{2,i}^{\text{eff}}} \right) \gamma_{th,A}^{J}. \tag{2.26}$$

2.2.3 Average BER Analysis

The average BER depends on the effective combiner output SNR of the source. Similar to the outage analysis, we will only derive the BER performance at source A. From (2.19), the effective SNR at the combiner output for A is the sum of effective SNRs on each relay branch from B to A. Under M-ary phase shifted keying modulation, the BER experienced by source A can be expressed as [35]

$$P_{e,A} = \frac{2}{\pi \log_2 M} \int_0^{\pi/2} \prod_{i=1}^{J} \mathcal{M}_{A,i}(s)\, \mathrm{d}\theta, \tag{2.27}$$

where $s := -\frac{g_{psk}}{\sin^2\theta}$, $g_{psk} := \sin^2(\pi/M)$, and $\mathcal{M}_{A,i}(\cdot)$ is the moment generating function (MGF) of the fading distribution contributed through the ith relay branch to source

[6] We write a function $f(x)$ of x as $o(x)$ if $\lim_{x\to 0} f(x)/x = 1$, and denote $f^{(n)}(0)$ as the nth order derivative of $f(x)$ evaluated at $x = 0$.

A. Therefore, we need the MGF expression of $\gamma_{A,i}^{\text{eff}}$ which is the harmonic mean of two exponentially distributed r.v.'s, $\gamma_{1,i}^{\text{eff}}$ and $\gamma_{2,i}^{\text{eff}}$, with means given in (2.17).

By using the closed-form MGF expression of the harmonic mean from [36, Theorem 4], the average BER in (2.27) can be derived as

$$P_{e,A} = \frac{2}{\pi \log_2 M} \int_0^{\frac{\pi}{2}} \prod_{i=1}^{J} \left(\frac{(\beta_{1,i} - \beta_{2,i})^2 + (\beta_{1,i} + \beta_{2,i}) \frac{g_{psk}}{\sin^2\theta}}{\Delta^2} + \frac{2\beta_{1,i}\beta_{2,i} g_{psk}}{\Delta^3 \sin^2\theta} \ln \frac{(\beta_{1,i} + \beta_{2,i} + \frac{g_{psk}}{\sin^2\theta} + \Delta)^2}{4\beta_{1,i}\beta_{2,i}} \right) \mathrm{d}\theta, \tag{2.28}$$

where $\Delta = \sqrt{(\beta_{1,i} - \beta_{2,i})^2 + 2(\beta_{1,i} - \beta_{2,i}) \frac{g_{psk}}{\sin^2\theta} + \left(\frac{g_{psk}}{\sin^2\theta}\right)^2}$.

Eq. (2.28) can be easily calculated via numerical integration. In order to see the effect of the system parameters more clearly, (2.28) can be approximated by an asymptotic bound given by

$$P_{e,A} \simeq \frac{2}{\pi \log_2 M} \int_0^{\frac{\pi}{2}} \frac{\sin^{2J}\theta}{\sin^{2J}(\pi/M)} \mathrm{d}\theta \prod_{i=1}^{J} \left(\frac{1}{\bar{\gamma}_{1,i}^{\text{eff}}} + \frac{1}{\bar{\gamma}_{2,i}^{\text{eff}}} \right) \tag{2.29}$$

by invoking the asymptotic property of [36, Theorem 4] together with the linearity of the MGF.

The BER at source B, $P_{e,B}$, can be obtained similarly. Finally, the average system BER can be described as $P_e = (P_{e,A} + P_{e,B})/2$.

2.3 *Max-Min* Relay Selection

Although all participating relaying as studied in Sec. 2.2 has been demonstrated to provide spatial diversity to combat wireless fading, it is of a lower achievable rate due to the use of orthogonal time slots in TDD mode. RS can be exploited to further improve the spectral efficiency while maintaining the spatial diversity. The optimal RS [12] should choose the relay minimizing the system BER as

$$i^* = \arg\min_i \{\text{BER}(\gamma_{A,i}^{\text{eff}} | \hat{h}_i, \hat{g}_i), \text{BER}(\gamma_{B,i}^{\text{eff}} | \hat{h}_i, \hat{g}_i)\}. \tag{2.30}$$

However, the optimal RS is hard to implement and its performance is analytically intractable. Since the system BER is typically dominated by the worse user, a suboptimal RS [12, 37] is proposed to minimize the higher BER in the pair sources, which

is formulated as

$$i^* = \arg\min_i \max\{\mathrm{BER}(\gamma_{A,i}^{\mathrm{eff}}|\hat{h}_i, \hat{g}_i), \mathrm{BER}(\gamma_{B,i}^{\mathrm{eff}}|\hat{h}_i, \hat{g}_i)\}. \tag{2.31}$$

The suboptimal RS in (2.31) can be further equivalently formulated in terms of the instantaneous effective received SNRs at sources as

$$i^* = \arg\max_i \min[\gamma_{A,i}^{\mathrm{eff}}, \gamma_{B,i}^{\mathrm{eff}}], \tag{2.32}$$

which is referred to as maximum minimum RS (*Max-Min RS*). The *Max-Min RS* chooses the "best relay" as one that maximizes the minimum of the two instantaneous effective SNRs for the pair sources, which coincides with the best-worse-channel selection [11,37]. Equivalently, the *Max-Min RS* minimizes the maximum error probability of two-way communication through the selected best-relay link rather than the average BER of the two sources. Comparing to other RS schemes, *Max-Min RS* not only achieves full diversity but is also easier to implement and achieves nearly the same BER performance as other RS schemes [11]. In this section, we examine the effect of imperfect CSI under the *Max-Min* single RS scheme to improve the rate performance.

2.3.1 Outage Probability Analysis for *Max-Min* RS

First, we determine the outage probability under the *Max-Min RS* when the channel estimation error exists. Since either $\gamma_{A,i}^{\mathrm{eff}} < 2^{2R_A} - 1$ or $\gamma_{B,i}^{\mathrm{eff}} < 2^{2R_B} - 1$ will cause a system outage, under the assumption that $R_A = R_B$ the overall system outage probability with this *Max-Min RS* scheme is

$$\begin{aligned} P_{out}^{RS} &= \Pr\left\{\min\left[\gamma_{A,i^*}^{\mathrm{eff}}, \gamma_{B,i^*}^{\mathrm{eff}}\right] < \gamma_{th}^{RS}\right\} \\ &= \prod_{i=1}^{J} \Pr\left\{\min\left[\gamma_{A,i}^{\mathrm{eff}}, \gamma_{B,i}^{\mathrm{eff}}\right] < \gamma_{th}^{RS}\right\} \\ &= \prod_{i=1}^{J} \left(\Pr\left\{\gamma_{A,i}^{\mathrm{eff}} < \gamma_{th}^{RS}\right\} + \Pr\left\{\gamma_{B,i}^{\mathrm{eff}} < \gamma_{th}^{RS}\right\}\right. \\ &\quad \left. - \Pr\left\{\gamma_{A,i}^{\mathrm{eff}} < \gamma_{th}^{RS}, \gamma_{B,i}^{\mathrm{eff}} < \gamma_{th}^{RS}\right\}\right), \end{aligned} \tag{2.33}$$

where $\gamma_{th}^{RS} = 2^{2R_A} - 1$ is the outage threshold, and $\Pr\{\gamma_{k,i}^{\mathrm{eff}} < \gamma_{th}^{RS}\} = 1 - e^{-\lambda_{k,i}\gamma_{th}^{RS}}$ for $k \in \{A, B\}$, and $Pr\left\{\gamma_{A,i}^{\mathrm{eff}} < \gamma_{th}^{RS}, \gamma_{B,i}^{\mathrm{eff}} < \gamma_{th}^{RS}\right\}$ is derived in Appendix A.

In the high SNR regime, we can approximate P_{out}^{RS} as $\prod_{i=1}^{J}(\Pr\left\{\gamma_{A,i}^{\text{eff}} < \gamma_{th}^{RS}\right\} + \Pr\left\{\gamma_{B,i}^{\text{eff}} < \gamma_{th}^{RS}\right\})$. Moreover, based on the fact that $\lim_{\mathcal{X}\to 0}(1 - e^{-\mathcal{X}}) = \mathcal{X}$, the asymptotic outage probability can be derived as

$$P_{out}^{RS} \simeq \prod_{i=1}^{J} \left(\left(1/\bar{\gamma}_{1,i}^{\text{eff}} + 1/\bar{\gamma}_{2,i}^{\text{eff}}\right)\gamma_{th}^{RS} + \left(1/\bar{\gamma}_{3,i}^{\text{eff}} + 1/\bar{\gamma}_{4,i}^{\text{eff}}\right)\gamma_{th}^{RS}\right). \tag{2.34}$$

2.3.2 Average BER Analysis for *Max-Min* RS

Define $P_{e,u}^{RS} = \max\{P_{e,\{A,i^*\}}, P_{e,\{B,i^*\}}\}$ as the higher BER of the two-way communication sources, where $P_{e,\{k,i^*\}}$ ($k \in \{A, B\}$) is the BER at source k when relay i^* is the best relay selected. Note that $P_{e,u}^{RS}$ is an upper bound of the exact average system BER given by $P_e^{RS} = (P_{e,\{A,i^*\}} + P_{e,\{B,i^*\}})/2$. Under the *Max-Min RS*, the upper bound $P_{e,u}^{RS}$ is minimized. In this subsection we derive the average BER upper bound expression for tractable analysis.

Conditioned on the instantaneous received SNR, the BER of a linear modulation format under AWGN can be approximated as $Q(\sqrt{c\gamma_{\mathcal{R}}})$ [38], where $Q(\cdot)$ is Gaussian-Q function, $Q(x) = \frac{1}{\sqrt{2\pi}}\int_x^\infty e^{-t^2/2}dt$, c is a constant determined by the modulation format, e.g., $c = 1$ for quadrature c shifted keying (QPSK) constellation, and $\gamma_{\mathcal{R}}$ represents the received SNR per symbol.

For the *Max-Min RS*, let $\gamma_{\mathcal{R}}$ denote the worse received SNR of the pair sources communicating through the selected best-relay link, formulated as $\gamma_{\mathcal{R}} = \max_i \min[\gamma_{A,i}^{\text{eff}}, \gamma_{B,i}^{\text{eff}}]$ where $i = 1, \cdots, J$. Since both $\gamma_{A,i}^{\text{eff}}$ and $\gamma_{B,i}^{\text{eff}}$ follow exponential distribution with the rate $\lambda_{A,i} = 1/\bar{\gamma}_{1,i}^{\text{eff}} + 1/\bar{\gamma}_{2,i}^{\text{eff}}$ and $\lambda_{B,i} = 1/\bar{\gamma}_{3,i}^{\text{eff}} + 1/\bar{\gamma}_{4,i}^{\text{eff}}$, the c.d.f. of $\gamma_{\mathcal{R}}$ can be easily derived from (2.33) as

$$\Pr\{\gamma_{\mathcal{R}} < s\} \simeq \prod_{i=1}^{J}(1 - e^{-(\lambda_{A,i}+\lambda_{B,i})s}). \tag{2.35}$$

Furthermore, under independent and identically distributed (i.i.d.) channel scenario for both sides of relays, $\lambda_{k,i}$ is the same for $i = 1, \cdots, J$, and hence denoted by λ_k, where $k \in \{A, B\}$. Thus,

$$\Pr\{\gamma_{\mathcal{R}} < s\} \simeq (1 - e^{-(\lambda_A+\lambda_B)s})^J. \tag{2.36}$$

By introducing a new r.v. with standard Normal distribution $X \sim \mathcal{N}(0, 1)$, the

average system BER upper bound can be rewritten as [39]

$$\begin{aligned} P_{e,u}^{RS} &= \Pr\{X > \sqrt{c\gamma_{\mathcal{R}}}\} = \Pr\left\{\gamma_{\mathcal{R}} < \frac{X^2}{c}\right\} = \mathbb{E}\left[F_{\gamma_{\mathcal{R}}}\left(\frac{X^2}{c}\right)\right] \\ &= \int_0^\infty F_{\gamma_{\mathcal{R}}}\left(\frac{X^2}{c}\right) f_X(x)\mathrm{d}x. \end{aligned} \tag{2.37}$$

By substituting (2.36) into (2.37) and using Binomial theorem to expand (2.36) and the fact that $\int_0^\infty e^{-q^2x^2}\mathrm{d}x = \sqrt{\pi}/2q$ [40], we obtain

$$\begin{aligned} P_{e,u}^{RS} &= \int_0^\infty (1 - e^{-(\lambda_A+\lambda_B)x^2/c})^J \frac{1}{\sqrt{2\pi}} e^{-x^2/2}\mathrm{d}x \\ &= \frac{1}{2\sqrt{2}} \sum_{k=0}^{J} \binom{J}{k} (-1)^k \left(\frac{(\lambda_A+\lambda_B)k}{c} + \frac{1}{2}\right)^{-1/2}. \end{aligned} \tag{2.38}$$

In the high SNR regime, we can also exploit the fact that $\lim_{\mathcal{X}\to 0}(1 - e^{-\mathcal{X}}) = \mathcal{X}$ to approximately calculate (2.35) as $\prod_{i=1}^{J}((\lambda_{A,i} + \lambda_{B,i})s)$. Recalling (2.37) and $X \sim \mathcal{N}(0,1)$, the asymptotic average BER upper bound can be written as

$$\begin{aligned} P_{e,u}^{RS} &\simeq \int_0^\infty \prod_{i=1}^{J} \left((\lambda_{A,i} + \lambda_{B,i})x^2/c\right) \frac{1}{\sqrt{2\pi}} e^{-x^2/2}\mathrm{d}x \\ &= \frac{(2J-1)!!}{2} \prod_{i=1}^{J} \left(\frac{\lambda_{A,i} + \lambda_{B,i}}{c}\right), \end{aligned} \tag{2.39}$$

where the last equation is based on the fact that $\int_0^\infty x^{2n} e^{-kx^2}\mathrm{d}x = \frac{(2n-1)!!}{2(2k)^n}\sqrt{\frac{\pi}{k}}$ [40].

2.4 Performance Enhancement by Adaptive Power Allocation

In this section, we show how performance degradation due to imperfect CSI can be mitigated by adaptive PA. We consider both cases of PA by minimizing either the outage probability or the average BER subject to both the total and individual power constraints. However, the minimization problems are not easy to solve due to the nonconvexity of the expressions in (2.24), (2.28), (2.33), and (2.38). In order to make the PA problem more tractable, we instead design the PA scheme by minimizing the asymptotic outage or BER expressions and use GP to address this.

2.4.1 Geometric programming

Geometric programming is a class of nonlinear, nonconvex optimization problem which can provide a global solution since it can be turned into a convex optimization problem [24–26]. In its *standard* form GP involves minimization of a monomial/posynomial[7] function subject to (s.t.) posynomial upper bound inequality and monomial equality constraints. The transformation to its *convex* form can be done with a logarithmic change of variables[8]. Then, recognizing that in its *convex* form GP is indeed convex since log-sum-exp function is convex [24, 25], GP can be readily solved by convex optimization technique [24]. For a greater in-depth look into the GP problems and its use in power control and communications problems please refer to [24–26].

2.4.2 Adaptive PA for Multiple Relays

By observing the asymptotic expressions of (2.26) and (2.29), we notice that both terms contain the form of $1/\bar{\gamma}_{1,i}^{\text{eff}} + 1/\bar{\gamma}_{2,i}^{\text{eff}}$, which is a generalized posynomial in terms of P_A, P_B, and P_{r_i}. Similar observation can be made to $P_{out}^B(\gamma_{th,B})$ and $P_{e,B}$ which all contain the term $1/\bar{\gamma}_{3,i}^{\text{eff}} + 1/\bar{\gamma}_{4,i}^{\text{eff}}$ that is again a posynomial in terms of P_A, P_B, and P_{r_i}. Then by introducing the auxiliary variables $(t_{A,i}, t_{B,i})$, and recognizing that posynomials are closed under addition, multiplication and positive scaling [24], the PA problem based on minimizing the asymptotic P_{out} approximated as $P_{out} = P_{out}^A + P_{out}^B$ or the average BER $P_e = (P_{e,A} + P_{e,B})/2$, subject to total and individual power

[7]From [24–26], a function is called *monomial* when it is defined as $f(\mathbf{x}) = dx_1^{a^{(1)}} x_2^{a^{(2)}} \cdots x_n^{a^{(n)}}$, where $d \geq 0$, and $a^{(j)} \in \mathbb{R}, j = 1, 2, \ldots, n$. On the other hand, a sum of monomials is called a *posynomial* and is given as $f(\mathbf{x}) = \sum_{k=1}^{K} d_k x_1^{a_k^{(1)}} x_2^{a_k^{(2)}} \cdots x_n^{a_k^{(n)}}$, where $d_k \geq 0$, $k = 1, \ldots, K$, and $a_k^{(j)} \in \mathbb{R}$, $j = 1, \ldots, n$, $k = 1, 2, \ldots, K$. Monomials are closed under multiplication and division; whereas, posynomials are closed under addition, multiplication and positive scaling [24], e.g., division of a posynomial by monomial is also a posynomial.

[8]From [24–26], a log transformation of variables to a posynomial $f(\mathbf{x})$ can be realized by substituting $x_i = e^{y_i}$ and $d_k = e^{b_k}$ into the expression and after some manipulations to obtain $p(\mathbf{y}) = \log \sum_{k=1}^{K} \exp(b_k + \mathbf{a}_k^T \mathbf{y})$, where $\mathbf{a}_k = [a_k^{(1)}, \ldots, a_k^{(n)}]^T$, $\mathbf{y} = [y_1, \ldots, y_n]^T$, and $(\cdot)^T$ denotes the transpose operation. The function $p(\mathbf{y})$ is now affine and is convex. Similar transformation can be applied to the objective function and its corresponding constraints. For more information please refer to [24–26].

constraints, can be formulated as

$$\begin{aligned}
&\min_{\{P_A,P_B,P_{r_i}\}} \left(\prod_{i=1}^{J} t_{A,i} + \prod_{i=1}^{J} t_{B,i}\right), \\
&\text{s.t. } (1/\bar{\gamma}_{1,i}^{\text{eff}} + 1/\bar{\gamma}_{2,i}^{\text{eff}})K_A \le t_{A,i},\ (1/\bar{\gamma}_{3,i}^{\text{eff}} + 1/\bar{\gamma}_{4,i}^{\text{eff}})K_B \le t_{B,i}, \\
&\quad P_A + P_B + \sum_{i=1}^{J} P_{r_i} \le P_{tot}, \\
&\quad 0 \le P_A \le P_A^{\text{MAX}}, 0 \le P_B \le P_B^{\text{MAX}}, 0 \le P_{r_i} \le P_{r_i}^{\text{MAX}},\ i = 1, \ldots, J, \\
&\quad t_{A,i} \ge 0, t_{B,i} \ge 0,\ i = 1, \ldots, J,
\end{aligned} \tag{2.40}$$

where P_{tot} and P_A^{MAX}, P_B^{MAX}, $P_{r_i}^{\text{MAX}}$ are upper bounds on system power and individual powers, and K_k ($k \in \{A, B\}$) is a constant and equal to $\gamma_{th,k}^{J}$ for outage probability or 1 for average BER. The optimization problem of (2.40) is a GP problem with optimization variables of P_A, P_B, P_{r_i}, $t_{A,i}$, and t_{B_i} in *standard* form, i.e., minimizing a posynomial objective function s.t. posynomial upper bound inequality, that can be transformed into its *convex* form [24–26] by a log transformation of variables, which can then be solved efficiently with convex optimization algorithm such as the `CVX` [27].

2.4.3 Adaptive PA for Max-Min RS

Similarly, based on the asymptotic expressions of (2.34) and (2.39), we can formulate the adaptive PA problem for *Max-Min RS* as the following GP problem in *standard* form

$$\begin{aligned}
&\min_{\{P_A,P_B,P_{\mathcal{R}}\}} \prod_{i=1}^{J} (t_{A,i} + t_{B,i}), \\
&\text{s.t. } (1/\bar{\gamma}_{1,i}^{\text{eff}} + 1/\bar{\gamma}_{2,i}^{\text{eff}})K_A \le t_{A,i}, (1/\bar{\gamma}_{3,i}^{\text{eff}} + 1/\bar{\gamma}_{4,i}^{\text{eff}})K_B \le t_{B,i}, \\
&\quad P_A + P_B + P_{\mathcal{R}} \le P_{tot}, \\
&\quad 0 \le P_A \le P_A^{\text{MAX}}, 0 \le P_B \le P_B^{\text{MAX}}, 0 \le P_{\mathcal{R}} \le P_{\mathcal{R}}^{\text{MAX}}, \\
&\quad t_{A,i} \ge 0, t_{B,i} \ge 0,\ i = 1, \ldots, J,
\end{aligned} \tag{2.41}$$

The constant K_k ($k \in \{A, B\}$) is equal to γ_{th}^{RS} for outage probability or $1/c$ for average BER. Once again (2.41) is GP in *standard* form that can be log transformed into the *convex* form and be solved efficiently by `CVX`.

2.5 Numerical Results and Discussion

This section provides numerical results to confirm the correctness of our theoretical analysis. We consider an uncoded QPSK system with either symmetric and asymmetric channels. With symmetric channels, the channels in between sources and relays are modeled as i.i.d. with an equal variance of 10, i.e., $\sigma_{h_i}^2 = \sigma_{g_i}^2 = 10$. In asymmetric channels case, the channels are only i.i.d. from one source to the relays while being distinct in between both sources to the relays and we let $\sigma_{h_i}^2 = 10$ and $\sigma_{g_i}^2 = 1$. In our simulations, we assume that the error variances are identical across all links, i.e., $\sigma_{e_{h_i}}^2 = \sigma_{e_{g_i}}^2 = \sigma_e^2$. Moreover, two different models for channel estimation error are used: 1) σ_e^2 is independent of the transmitted SNR, and 2) σ_e^2 is a decreasing function of both SNR and the length of training sequences K, formulated as $\sigma_e^2 = \frac{1}{K \cdot \text{SNR}}$ [28]. We further assume that the noise components are i.i.d. with common variance, i.e., $N_{r_i} = N_{A,i} = N_{B,i} = 1$, and the target transmission rates are $R_A = R_B = 1$ bit per second per Hz. The results shown are averaged over 1,000 independent trials.

When employing multiple relays, we compare the outage and BER analytical expressions against simulation for both symmetric and asymmetric channels cases in Figs. 2.2 through 2.5. The σ_e^2 is assumed to take values of 0.01 and 0.001 in Figs. 2.2 to 2.4, and be a deceasing function of the transmitted SNR in Fig. 2.5. The result of these simulations show that our analysis matches well with the simulation results and adaptive PA significantly outperforms that of equal PA in asymmetric channels case. We would like to note that Fig. 2.2 includes both outage and BER and contains only the equal PA results since the performance gain from adaptive PA is limited due to the symmetry of the channels. We also plot the performances with perfect CSI, and observe that the imperfect CSI brings forth irreducible error floor at high SNR as illustrated in Figs. 2.2 through 2.4, when σ_e^2 is modeled as a constant. As shown in Fig. 2.5, when σ_e^2 is modeled as SNR and K dependent, i.e., $\sigma_e^2 = \frac{1}{K \cdot \text{SNR}}$, we observe both the outage and BER performance with and without the channel estimation error are deceasing as a function of the transmitted SNR but preserving a gap, irrespective of the SNR. This performance gap results from the SNR loss due to the estimation error. The observation of the irreducible error floor in Figs. 2.2 through 2.4 and preserved performance gap in Fig. 2.5 agrees with the previous results in OWRN [15, 16].

In Figs. 2.6 and 2.7, we plot outage probability and average BER for different number of relays with a fixed σ_e^2 of 0.001. It is not surprising to observe that using

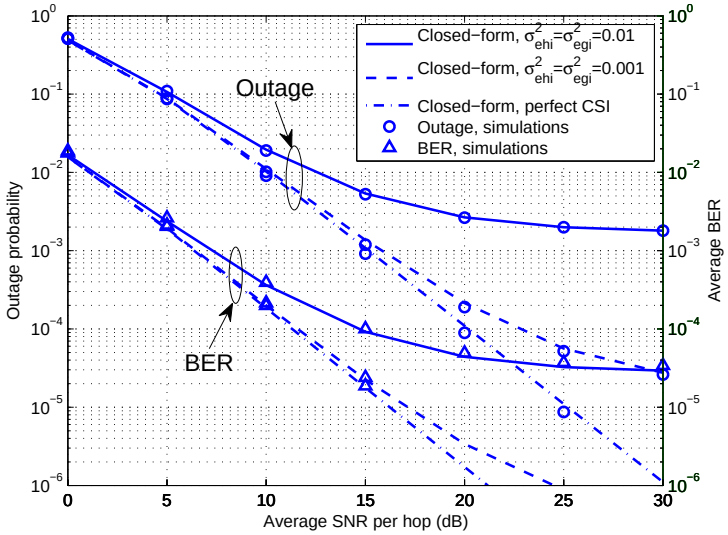

Figure 2.2: Outage Probability and average BER of AF TWRN with two relays using QPSK modulation. The channels of two relay links are symmetric with variance of 10. Only equal PA is considered.

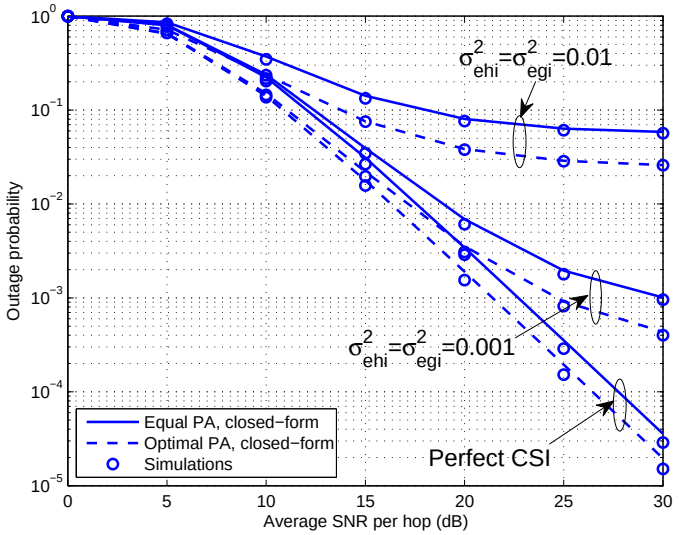

Figure 2.3: Outage probability of AF TWRN with two relays. The channels of both sides of the relays are i.i.d. with variances of 10 between A and R_i and 1 between B and R_i.

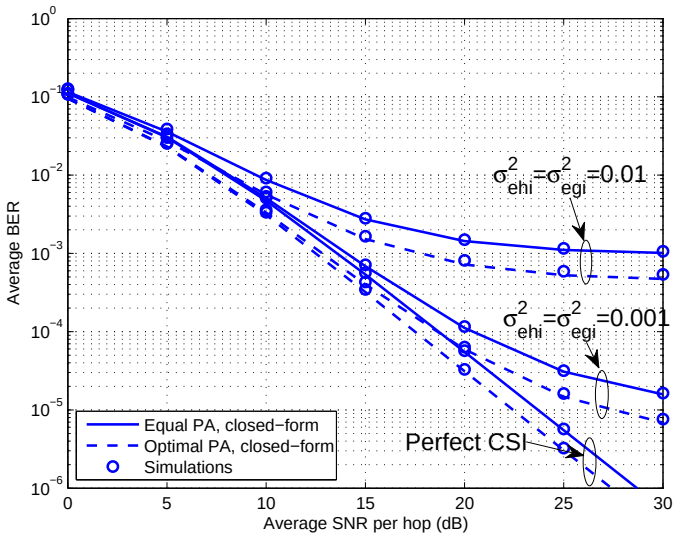

Figure 2.4: Average BER of AF TWRN with two relays using QPSK modulation. The channels of both sides of the relays are i.i.d. with variances of 10 between A and R_i and 1 between B and R_i.

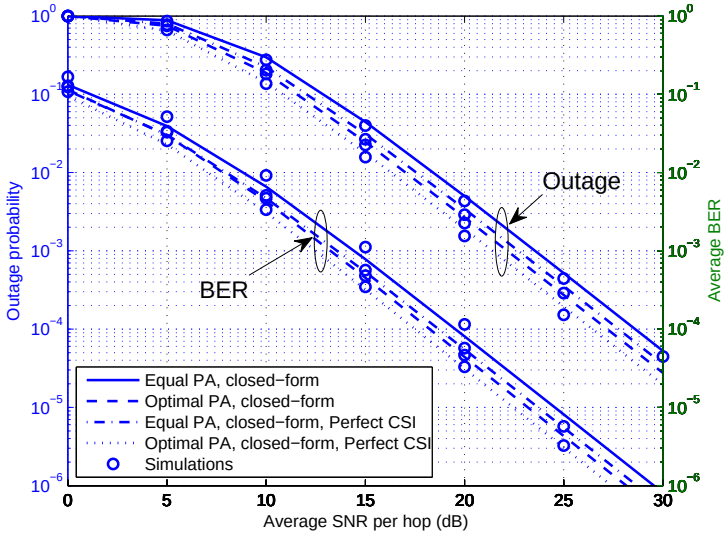

Figure 2.5: Outage Probability and average BER of AF TWRN with two relays using QPSK modulation. The channels of both sides of the relays are i.i.d. with variances of 10 between A and R_i and 1 between B and R_i, and $\sigma_e^2 = \frac{1}{K \cdot SNR}$ with $K = 10$.

more relays achieves a better performance, especially for medium SNRs in which adding more relays can provide a steeper decaying slope. However, these performance gains diminish due to the irreducible error floor from CSI error, which ultimately results in a zero diversity order at high SNR. However, when the channel estimation error is modeled as a decreasing function of the transmitted SNR, then the system achieves the same diversity order as in the perfect CSI as illustrated in Fig. 2.5.

Figs. 2.8 and 2.9 illustrate the system outage probability and BER performance of *Max-Min RS* under both adaptive and equal PA schemes for σ_e^2 of 0.01, and 0.001. By comparing with that of perfect CSI, we observe similarity to the multiple relay case, namely the irreducible error floor at high SNR. However, comparing between Figs. 2.3 and 2.8, under perfect CSI we observe that adaptive PA achieves 1 dB gain over equal PA with multiple relays while 3 dB gain with *Max-Min RS* at an outage probability of 10^{-3}. Similar trend in performance can also be observed for the BER. It should be noted that a small gap between the theoretical results and simulations can be observed in Fig. 2.9. However, the theoretical analysis indicates the general trends in average BER which are consistent with the simulations.

Finally, the processing time for the `CVX` algorithm is shown in Table 2.1. It takes seconds to implement PA for a two-relay network, and about 10 seconds for a 8-relay network. The efficiency of solving GP has also been studied in [24], indicating that the standard interior-point algorithms can solve a GP with 1,000 variables and 10,000 constraints in under a minute, on a small desktop computer. Note that the power allocation algorithm is based on average channel statistics (not the instantaneous channel realization) which does not change quickly with time. So the deployment of the `CVX` algorithm to implement PA as a GP problem is feasible in practical scenarios to enhance the system performance.

Table 2.1: Average processing time for the `CVX` algorithm based on 2.4 GHz Intel Core 2 Duo processor. The channels of both sides of the relays are i.i.d. with variances of 10 between A and R_i and 1 between B and R_i, and $\sigma_e^2 = 0.001$.

# of Relays	2	4	8
Average Time (sec.)	3.7637	5.7631	10.1362

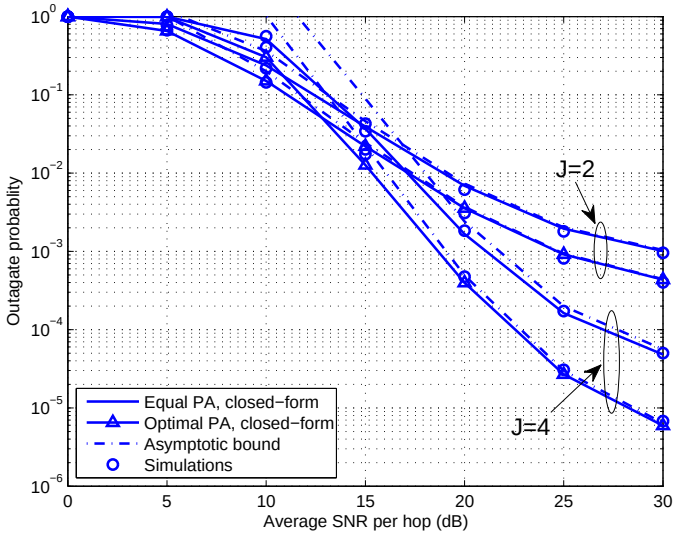

Figure 2.6: Outage Probability of AF TWRN with multiple relays. The channels of both sides of the relays are i.i.d. with variances of 10 between A and R_i and 1 between B and R_i, and $\sigma_e^2 = 0.001$.

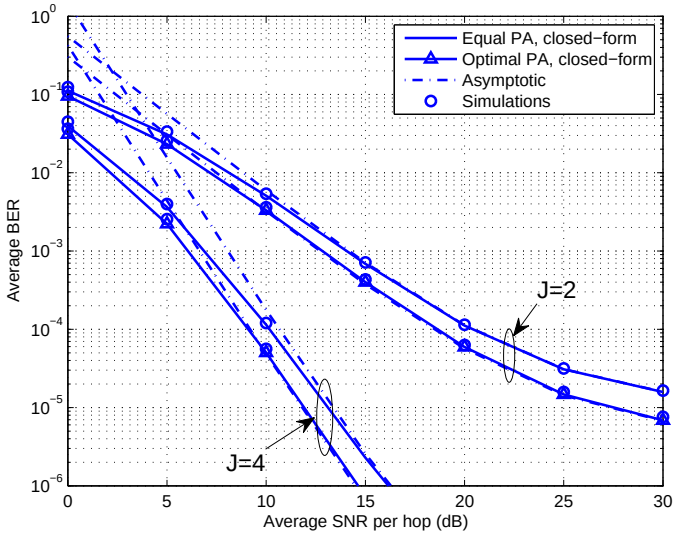

Figure 2.7: Average BER of AF TWRN with multiple relays using QPSK modulation. The channels of both sides of the relays are i.i.d. with variances of 10 between A and R_i and 1 between B and R_i, and $\sigma_e^2 = 0.001$.

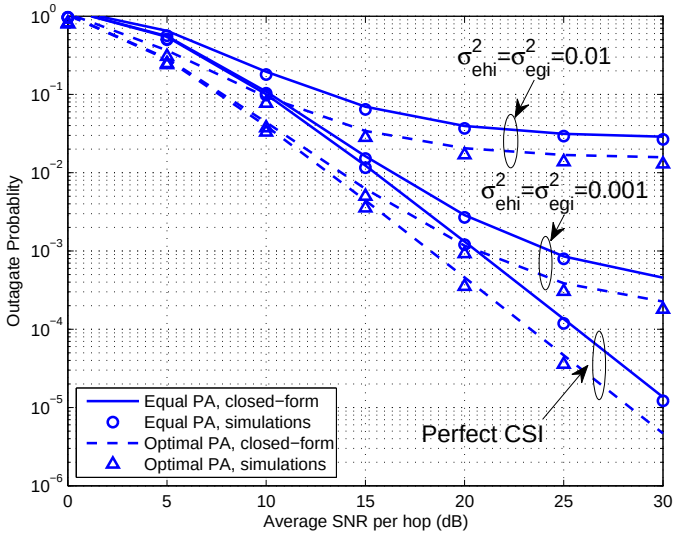

Figure 2.8: Outage Probability of AF TWRN with two relays for *Max-Min RS*. The channels of both sides of the relays are i.i.d. with variances of 10 between A and R_i and 1 between B and R_i.

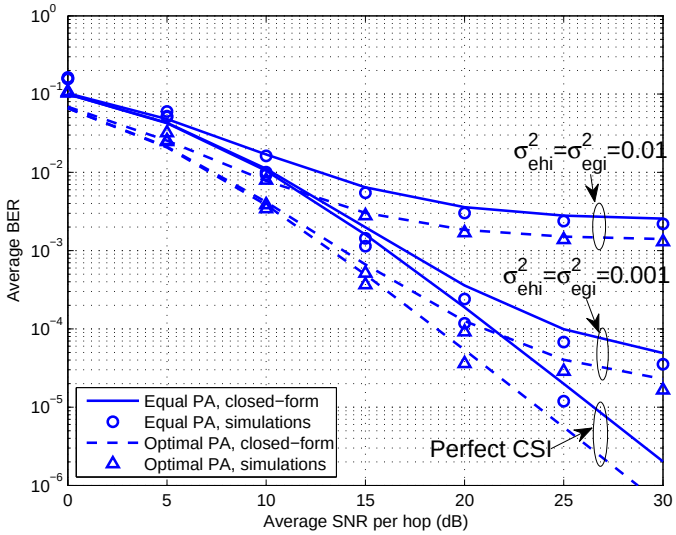

Figure 2.9: Average BER of AF TWRN with two relays for *Max-Min RS* using QPSK modulation. The channels of both sides of the relays are i.i.d. with variances of 10 between A and R_i and 1 between B and R_i.

2.6 Conclusions

In this chapter we have provided both the outage probability and BER analysis of multi-relay bidirectional AF protocol in the presence of channel estimation error. We have derived both outage probability and BER bounds which prove to be tight at high SNR. Based on the derived performance bounds, we have performed PA among all the nodes in the network that minimizes both outage probability and BER bounds with imperfect CSI. Single relay selection has also been taken into consideration to improve the system performance, and its degradation due to imperfect CSI has been examined. We have shown that the adaptive PA by GP provides substantial performance enhancement as compared to the equal PA scheme.

Chapter 3

Robust MIMO Relay Design for Two-Way MIMO Relaying with Imperfect CSI

In this chapter, we introduce the MIMO relay into the AF TWRN, and consider a system consisting of a pair of communicating single-antenna sources and a single multi-antenna relay under imperfect CSI condition. It is assumed that the MIMO relay has obtained channel estimates of both backward and forward channels to perform the robust precoder design, and the source has the knowledge of an estimate of its own channels so that it can perform self-interference cancellation. We take into account both the imperfect self-interference cancellation and imperfect data detection due to the CSI estimation error. To simplify the analysis and design, we further assume that the powers of CSI estimation error with exponent larger than 1 are negligible because in reality the CSI estimation error is usually small. Based upon all these assumptions, we propose a robust design of the AF MIMO relay precoder for the TWRN with imperfect CSI at both sources and relay. By using the worst-case approach [41], the transmit power at the relay is minimized while fulfilling the SNR constraints at both sources. This approach is widely used in robust MIMO relay designs for downlink broadcast channel [42, 43], single-user or multiuser MIMO system [44, 45], and one-way MIMO relaying system [21–23]. The design optimization problem turns out to be nonconvex. However, we utilize the SDR technique to reformulate this robust MIMO relay design problem as a convex optimization problem with second-order cone (SOC) program and semidefinite cone constraints, solved efficiently by means of

well established convex programming technique. Since the feasible set of the natural optimization problem is a subset of that of SDR-based problem, the randomization procedure is then applied to obtain an approximate solution of the original program. To this end, the SDR-based approximation method successfully derives the precoder matrix of the MIMO relay by minimizing the relay power and meanwhile maintaining the SNR at both sources above a threshold value in the worst-case sense.

The remainder of the chapter is organized as follows. Sec. 3.1 introduces the system model under consideration. Sec. 3.2 presents the channel uncertainty model as well as the optimization formulation with imperfect CSI. The robust design of the MIMO relay in the presence of channel estimation error is proposed in Sec. 3.3, and the semidefinite relaxation as well as the randomization technique are exploited to solve the optimal MIMO relay precoder. Numerical results are given in Sec. 3.4, and Sec. 3.5 concludes this chapter.

Notation: Boldface uppercase/lowercase letters denote matrices/vectors. The superscripts $(\cdot)^T$ and $(\cdot)^H$ denote transpose and Hermitian transpose. $\mathrm{tr}(\cdot)$, $\mathrm{vec}(\cdot)$, $\|\cdot\|$, and $\mathrm{rank}(\cdot)$ denote the trace, the vectorization, the Euclidean norm, and the rank operators, respectively. $\otimes$, $\odot$, $\mathcal{R}\{\}$, and $\mathcal{I}\{\}$ denote Kronecker product, elementwise product, the real part and the imaginary part, respectively. By $\mathbf{X} \succeq 0$ we denote that $\mathbf{X}$ is a Hermitian positive-semidefinite matrix. Finally, $\mathbf{I}_N$, $\mathbf{1}_{1\times N}$, and $\mathcal{C}^{N\times N}$ denote the $N \times N$ identity matrix, the all-ones column vector, and the space of $N \times N$ matrices with complex entries, respectively.

3.1 System Model

We consider a two-way AF relay-assisted system consisting of two sources A and B exchanging information with the help of a single relay with multiple antennas. As shown in Fig. 3.1, each source is equipped with a single antenna while the relay has N antennas, but all are operated under half-duplex mode so that they cannot transmit and receive at the same time. There is no direct link between A and B. We assume that the TWRN is a TDD system, which means both the uplink and downlink channels occupy the same frequency slot, but are differentiated in a time duplex manner in information exchange.

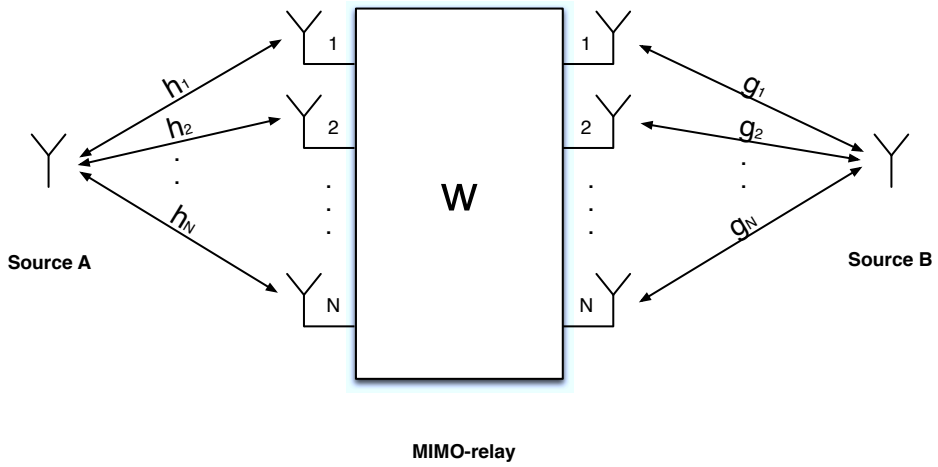

Figure 3.1: System model for AF two-way MIMO relay network.

3.1.1 Data Model

In the ANC-based system herein, we consider a two-phase cooperative strategy where the first phase involves the pair of sources transmitting simultaneously. At the MIMO relay, the received sum signal is linearly processed and then broadcasted in the second phase. Since TDD is assumed, the signal received at the relay station in the first time slot is

$$\mathbf{r}_R = \mathbf{h}x_A + \mathbf{g}x_B + \mathbf{n}_R, \tag{3.1}$$

where x_A and x_B denote the transmitted signals with unit average energy, i.e., $\mathbb{E}[|x_A|^2] = 1$ and $\mathbb{E}[|x_B|^2] = 1$, and the unit transmit power is assumed at both sources A and B. Variables $\mathbf{h} = [h_1, \ldots, h_N]^T$ and $\mathbf{g} = [g_1, \ldots, g_N]^T$ are discrete baseband equivalent channel coefficient vectors for both sides of the link to the MIMO relay, as indicated in Fig. 3.1. Vector $\mathbf{n}_R = [n_R^{(1)}, \ldots, n_R^{(N)}]^T$ is circularly symmetric AWGN at the relay antennas. Each entry of $\mathbf{n}_R$ is independent and modeled as CGRV with zero-mean and the same variance N_R, i.e., $\mathbf{n}_R \sim \mathcal{CN}(\mathbf{0}, N_R\mathbf{I}_N)$.

We assume that both uplink (from source to relay) and downlink (from relay to source) CSI are available at the relay station to serve the precoder design. The relay can employ the pilots from both sources to estimate the uplink channels, and use them as estimates in the downlink due to the channel reciprocity principle. In the

second time slot, the relay linearly processes the received signal by multiplying it with the precoder matrix $\mathbf{W}$, and then forwards the following signal to the sources,

$$\mathbf{s}_R = \mathbf{W} \cdot \mathbf{r}_R. \tag{3.2}$$

Note that the transmit power at the MIMO relay can be derived from (3.2) as

$$\begin{aligned} P_R &= \mathrm{tr}\left(\mathbb{E}[\mathbf{s}_R \mathbf{s}_R^H]\right) \\ &= \mathrm{tr}\left(\mathbf{W}\left(\mathbf{h}\mathbf{h}^H + \mathbf{g}\mathbf{g}^H + N_R \mathbf{I}_N\right)\mathbf{W}^H\right), \end{aligned} \tag{3.3}$$

where $\mathbb{E}[x_k x_k^H] = 1$ ($k \in \{A, B\}$), and $\mathbb{E}[\mathbf{n}_R \mathbf{n}_R^H] = N_R \mathbf{I}_N$. The signals received by the two sources in scalar form are

$$y_A = \mathbf{h}^T \mathbf{s}_R + n_A = \underbrace{\mathbf{h}^T \mathbf{W} \mathbf{g} x_B}_{\text{Signal Part}} + \underbrace{\mathbf{h}^T \mathbf{W} \mathbf{h} x_A}_{\text{Self-interference}} + \underbrace{\mathbf{h}^T \mathbf{W} \mathbf{n}_R + n_A}_{\text{Noise Part}}, \tag{3.4a}$$

$$y_B = \mathbf{g}^T \mathbf{s}_R + n_B = \underbrace{\mathbf{g}^T \mathbf{W} \mathbf{h} x_A}_{\text{Signal Part}} + \underbrace{\mathbf{g}^T \mathbf{W} \mathbf{g} x_B}_{\text{Self-interference}} + \underbrace{\mathbf{g}^T \mathbf{W} \mathbf{n}_R + n_B}_{\text{Noise Part}}, \tag{3.4b}$$

where n_A and n_B denote the AWGN with variance N_A and N_B, respectively. Let $\hat{\mathbf{h}}$ and $\hat{\mathbf{g}}$ denote the channel estimates. We assume the relay forwards CSI estimates as well as the precoder matrix $\mathbf{W}$ to the sources through the feedback channels. The quantization error as well as the error in the feedback channels is not considered in this chapter. So the CSI estimates used for the source-relay reciprocal channels are identical, and the sources have a copy of $\mathbf{W}$ for the further process of the received signal. Then the self-interference can be cancelled as $z_A = y_A - \hat{\mathbf{h}}^T \mathbf{W} \hat{\mathbf{h}} x_A$ and $z_B = y_B - \hat{\mathbf{g}}^T \mathbf{W} \hat{\mathbf{g}} x_B$. If perfect channel condition is assumed, the self-interference can be totally removed since the sources know their own transmitted data. For the imperfect CSI case, however, the self-interference cannot be completely subtracted due to the fact that the channel estimates are not always equal to the actual channel in practice. To this end, we consider the case where the imperfect self-interference cancellation will lead to residual self-interference, although it is shown later in this chapter that the residual self-interference can be ignored based upon some assumption.

For the convenience of future analysis, define $\mathbf{H}_{DL} = [\mathbf{g}\ \mathbf{h}]^T$ and $\mathbf{H}_{UL} = [\mathbf{h}\ \mathbf{g}]$,

and we can represent both (3.4a) and (3.4b) in an equivalent matrix form as

$$\mathbf{y} = \mathbf{H}_{DL}\mathbf{W}\mathbf{H}_{UL}\mathbf{x} + \mathbf{H}_{DL}\mathbf{W}\mathbf{n}_R + \mathbf{n} \tag{3.5}$$

where $\mathbf{y} = [y_B \; y_A]^T$, $\mathbf{x} = [x_A \; x_B]^T$, and $\mathbf{n} = [n_B \; n_A]^T$.

3.1.2 Problem Formulation under Perfect CSI

The design of MIMO relay precoder is based upon providing the QoS assurance for both sources. The QoS is usually measured in terms of SNR, which determines the maximum achievable data rate and essentially determines the BER. There are two design criteria widely considered in the literature [46, 47] – QoS and max-min fair (MMF). The QoS-guaranteed design is to minimize the transmit power at the relay station while providing a guaranteed minimum received SNR to both sources, while MMF design problem is to maximize the minimum received SNR of two sources subject to a bound on the transmitted power at the MIMO relay. Both have been proved NP-hard [46, 47]. For the single-group multicast problem which is essentially involved in the second time slot of MIMO relay broadcasting the linear processed received signal, it has been theoretically shown that the two design formulations of QoS-guaranteed and MMF are algorithmically equivalent [47], i.e., an optimal algorithm that provides the exact solution to one could be used to obtain the exact solution to the other. In this thesis, we resort to the QoS-guaranteed method to design the MIMO relay.

In this subsection, we will present a quick review of the optimal MIMO relay structure in the perfect CSI case. The SNR at the source is derived, and then the power minimization problem under SNR constraints is formulated. Similar work has been done in [17], and an efficient algorithm is also provided to compute the optimal precoder matrix. But the design in [17] is based on the ideal situation where perfect CSI is available, which we will refer to as the nonrobust method in the following chapter. The nonrobust precoder structure will provide us a baseline for our robust design, and some comparison will be given in Sec. 3.4. In this chapter, we only mathematically analyze the transmission from B to A, and similar method can be applied to that from A to B.

First, the following operation is defined to convert a column vector $\mathbf{f} = [f_1, \ldots, f_N]^T$

with N entries to two new row vectors $\tilde{\mathbf{f}}_1$ and $\tilde{\mathbf{f}}_2$ with N^2 entries each as

$$\begin{aligned}\tilde{\mathbf{f}}_1 &= \mathbf{f}^T \left(\mathbf{I}_N \otimes \mathbf{1}_{1\times N}\right)_{N\times N^2} \triangleq \mathbf{f}^T\mathbf{D}_1 = [f_1 \cdots f_1 \ \cdots \ f_N \cdots f_N],\\ \tilde{\mathbf{f}}_2 &= \mathbf{f}^T \left(\mathbf{1}_{1\times N} \otimes \mathbf{I}_N\right)_{N\times N^2} \triangleq \mathbf{f}^T\mathbf{D}_2 = [f_1 \cdots f_N \ \cdots \ f_1 \cdots f_N].\end{aligned} \tag{3.6}$$

So the received signal at source A in (3.4a) can be rewritten as

$$y_A = (\tilde{\mathbf{g}}_1 \odot \tilde{\mathbf{h}}_2)\mathbf{w}_L x_B + (\tilde{\mathbf{h}}_1 \odot \tilde{\mathbf{h}}_2)\mathbf{w}_L x_A + (\tilde{\mathbf{n}}_{R,1} \odot \tilde{\mathbf{h}}_2)\mathbf{w}_L + n_A, \tag{3.7}$$

where $\tilde{\mathbf{h}}_1 = \mathbf{h}^T\mathbf{D}_1$, $\tilde{\mathbf{h}}_2 = \mathbf{h}^T\mathbf{D}_2$, $\tilde{\mathbf{g}}_1 = \mathbf{g}^T\mathbf{D}_1$, $\tilde{\mathbf{n}}_{R,1} = \mathbf{n}_R\mathbf{D}_1$, and $\mathbf{w}_L = \text{vec}(\mathbf{W})$. Note that the vec($\mathbf{W}$) operation stacks the columns of $\mathbf{W}$ each by each, and finally converts the matrix $\mathbf{W}$ to a column vector as $[w_{11}\ w_{21}\cdots w_{N1}\ \cdots\ w_{1N}\ w_{2N}\cdots w_{NN}]^T$. After cancelling the self-interference, the signal at source A becomes

$$\begin{aligned} z_A &= y_A - \hat{\mathbf{h}}^T\mathbf{W}\hat{\mathbf{h}}x_A \\ &= \underbrace{(\tilde{\mathbf{g}}_1 \odot \tilde{\mathbf{h}}_2)\mathbf{w}_L x_B}_{\text{Signal part } r_A} + \underbrace{(\tilde{\mathbf{n}}_{R,1} \odot \tilde{\mathbf{h}}_2)\mathbf{w}_L + n_A}_{\text{Noise part } t_n} + \underbrace{\left((\tilde{\mathbf{h}}_1 \odot \tilde{\mathbf{h}}_2) - (\hat{\tilde{\mathbf{h}}}_1 \odot \hat{\tilde{\mathbf{h}}}_2)\right)\mathbf{w}_L x_A}_{\text{Interference part } t_s}. \end{aligned} \tag{3.8}$$

The received SNR at source A after self-interference cancellation is obtained as

$$\gamma_A = \frac{\mathbf{w}_L^H \left(\tilde{\mathbf{g}}_1 \odot \tilde{\mathbf{h}}_2\right)^H \left(\tilde{\mathbf{g}}_1 \odot \tilde{\mathbf{h}}_2\right)\mathbf{w}_L}{t_n + t_s} \triangleq \frac{r_A}{s_A} \tag{3.9}$$

where

$$\begin{aligned} t_n &= \mathbf{w}_L^H \left(\mathbf{N}^r \odot \left(\tilde{\mathbf{h}}_2^H\tilde{\mathbf{h}}_2\right)\right)\mathbf{w}_L + \sigma_{n_A}^2, \text{and} \\ t_s &= \mathbf{w}_L^H \left(\tilde{\mathbf{h}}_1 \odot \tilde{\mathbf{h}}_2\right)^H \left(\tilde{\mathbf{h}}_1 \odot \tilde{\mathbf{h}}_2\right)\mathbf{w}_L + \mathbf{w}_L^H \left(\hat{\tilde{\mathbf{h}}}_1 \odot \hat{\tilde{\mathbf{h}}}_2\right)^H \left(\hat{\tilde{\mathbf{h}}}_1 \odot \hat{\tilde{\mathbf{h}}}_2\right)\mathbf{w}_L \\ &\quad - \mathbf{w}_L^H \left(\tilde{\mathbf{h}}_1 \odot \tilde{\mathbf{h}}_2\right)^H \left(\hat{\tilde{\mathbf{h}}}_1 \odot \hat{\tilde{\mathbf{h}}}_2\right)\mathbf{w}_L - \mathbf{w}_L^H \left(\hat{\tilde{\mathbf{h}}}_1 \odot \hat{\tilde{\mathbf{h}}}_2\right)^H \left(\tilde{\mathbf{h}}_1 \odot \tilde{\mathbf{h}}_2\right)\mathbf{w}_L. \end{aligned} \tag{3.10}$$

Note that $\mathbf{N}^r = \mathbb{E}[(\tilde{\mathbf{n}}_{R,1})^H\tilde{\mathbf{n}}_{R,1}] \in \mathcal{C}^{N^2\times N^2}$, which can also be expressed as $\mathbf{N}^r = N_R(\mathbf{I}_N \otimes \mathbf{1}_{N\times N})$. Since the perfect channel is assumed, the self-interference can be completely removed and therefore t_s in (3.10) is equal to zero.

Also, by using the identical transformation as shown in (3.12) the transmit power

in (3.3) can be further rewritten in terms of $\mathbf{w}_L$ and $\mathbf{H}_{UL}$ as

$$\begin{aligned} P_R &= \mathrm{tr}\left(\mathbf{W}^H\mathbf{W}\left(\mathbf{H}_{UL}\mathbf{H}_{UL}^H + \sigma_{n_R}^2\mathbf{I}_N\right)\right) \\ &\overset{(a)}{=} \mathrm{tr}\left(\mathbf{W}\left(\mathbf{H}_{UL}\mathbf{H}_{UL}^H + \sigma_{n_R}^2\mathbf{I}_N\right)\mathbf{W}^H\right) \\ &\overset{(b)}{=} \mathrm{vec}\left(\mathbf{W}\right)^H \mathrm{vec}\left(\mathbf{W}\left(\mathbf{H}_{UL}\mathbf{H}_{UL}^H + \sigma_{n_R}^2\mathbf{I}_N\right)\right) \\ &\overset{(c)}{=} \mathrm{vec}\left(\mathbf{W}\right)^H \left(\left(\mathbf{H}_{UL}\mathbf{H}_{UL}^H + \sigma_{n_R}^2\mathbf{I}_N\right)^T \otimes \mathbf{I}_N\right) \mathrm{vec}\left(\mathbf{W}\right) \\ &\triangleq \mathbf{w}_L^H\mathbf{C}\mathbf{w}_L, \end{aligned} \tag{3.11}$$

where the identical transformation in each step are provided as

$$\begin{aligned} &(a) \quad \mathrm{tr}\left(\mathbf{AB}\right) = \mathrm{tr}\left(\mathbf{BA}\right), \\ &(b) \quad \mathrm{tr}\left(\mathbf{A}^H\mathbf{B}\right) = \mathrm{vec}\left(\mathbf{A}\right)^H \mathrm{vec}\left(\mathbf{B}\right), \\ &(c) \quad \mathrm{vec}\left(\mathbf{AB}\right) = \left(\mathbf{B}^T \otimes \mathbf{I}\right) \mathrm{vec}\left(\mathbf{A}\right). \end{aligned} \tag{3.12}$$

Now, the optimal precoder design with the actual channel knowledge at the relay can be formulated as the optimization problem with the objective of minimizing the transmit power at the relay and constraints of satisfying the prescribed SNR threshold value at both sources, i.e.,

$$\begin{aligned} &\mathcal{P}^{nrob} : \min_{\mathbf{w}_L} P_R \\ &\text{s.t. } \gamma_k \geq \gamma_{th}, \ k \in \{A, B\}. \end{aligned} \tag{3.13}$$

It should be noted that $\mathcal{P}^{nrob}$ is not always feasible especially when the target SNR value is set too high [46, 48].

Back to the main concern of this chapter, it's too optimistic to assume the precise knowledge of CSI at the relay, and estimation errors should be taken into account to guarantee the robustness of MIMO relay design. Hence, the channel uncertainty ought to be incorporated to both objective and constrains in (3.13), and modeling the channel uncertainty along with the problem of designing the robust MIMO relay is investigated in the following two sections.

3.2 Channel Uncertainty Model

In the aforementioned system, the CSI is estimated once at the MIMO relay, and then forwarded to both sources through the feedback channels. We assume that the feedback channel is error-free and has low delay, and that the quantization of the channel estimates at the relay is perfect. So AWGN is the main source of CSI error, which is referred to as channel uncertainty in the following part of this chapter. It should be noted that different from one-way relaying where the downlink CSI is fed back from the destination to the MIMO relay [21–23], the MIMO relay here uses the uplink CSI estimates as that of downlink to design the precoder since the uplink and downlink is reciprocal to each other.

Let the estimates of the channel coefficients for both links to the MIMO relay be $\hat{\mathbf{h}} = [\hat{h}_1, \ldots, \hat{h}_N]^T$ and $\hat{\mathbf{g}} = [\hat{g}_1, \ldots, \hat{g}_N]^T$. We assume that both entry pairs h_i, $\hat{h}_i$ and g_i, $\hat{g}_i$ can be modeled as jointly ergodic and stationary Gaussian processes. The relations between the actual channels and the estimated channels are given by

$$\mathbf{h} = \hat{\mathbf{h}} + \mathbf{e}_h, \text{and } \mathbf{g} = \hat{\mathbf{g}} + \mathbf{e}_g, \tag{3.14}$$

where the channel estimation errors are $\mathbf{e}_h = [e_h^{(1)}\ e_h^{(2)}\ \cdots\ e_h^{(N)}]^T$ and $\mathbf{e}_g = [e_g^{(1)}\ e_g^{(2)}\ \cdots\ e_g^{(N)}]^T$. We consider the entries of $\mathbf{e}_h$ and $\mathbf{e}_g$ are i.i.d. following the distribution of $\mathcal{CN}(0, \sigma_{e_h}^2)$ and $\mathcal{CN}(0, \sigma_{e_g}^2)$, respectively.

We further assume that both $\mathbf{e}_h$ and $\mathbf{e}_g$ are norm-bounded as

$$\|\mathbf{e}_h\| \leq \delta_h, \text{and } \|\mathbf{e}_g\| \leq \delta_g, \tag{3.15}$$

where $\|\cdot\|$ denotes the Euclidean norm of a vector. Equivalently, the uncertainty region for each channel can be specified as [44]

$$\begin{aligned} \mathcal{R}_{\mathbf{h}} &= \{\zeta | \zeta = \hat{\mathbf{h}} + \mathbf{e}_h, \|\mathbf{e}_h\| \leq \delta_h\}, \\ \text{and} \quad \mathcal{R}_{\mathbf{g}} &= \{\zeta | \zeta = \hat{\mathbf{g}} + \mathbf{e}_g, \|\mathbf{e}_g\| \leq \delta_g\}. \end{aligned} \tag{3.16}$$

The relation between error variance and upper bound of the norm is also discussed in [44]. A more definite mathematical method is provided in [21] to determine $\delta_h(\delta_g)$ from $\sigma_{e_h}^2(\sigma_{e_g}^2)$ by means of numerical search, which will be summarized with δ_h and $\sigma_{e_h}^2$ as an example.

Let T be a r.v. following the chi-square distribution with N degrees of freedom,

and its p.d.f. is given by [49]

$$f_T(t,N) = \frac{1}{2^{N/2}\Gamma(N/2)} v^{N/2-1} e^{-v/2}. \tag{3.17}$$

Define $\|\mathbf{e}_h\|^2 = \sigma_{e_h}^2 T$, then the outage probability of the received SNR is shown equal to $1 - \Pr\{\sigma_{e_h}^2 T \leq \delta_h\}$ [44]. $\Pr\{\sigma_{e_h}^2 T \leq \delta_h^2\}$ is some predefined bounding probability and given by

$$\begin{aligned} \Pr\{\sigma_{e_h}^2 T \leq \delta_h^2\} &= \int_0^{\delta_h^2/\sigma_{e_h}^2} f_T(t,N)\mathrm{d}t \\ &= \frac{1}{\Gamma(N/2)} \gamma\left(\frac{N}{2}, \frac{\delta_h^2}{2\sigma_{e_h}^2}\right), \end{aligned} \tag{3.18}$$

where $\Gamma(\cdot)$ and $\gamma(\cdot)$ are the complete and lower complete Gamma functions, respectively. So given the predefined outage probability and estimation error variance, the upper bound of the norm of the channel uncertainty can be numerically determined.

Generally speaking, the channel estimation error is much smaller compared to the actual channel, so it is reasonable to not take the second-order terms of $\mathbf{e}_h$ and $\mathbf{e}_g$ and their cross-product into account. By applying the operation in (3.6) to the channel estimates vectors, $\hat{\mathbf{h}}$ and $\hat{\mathbf{g}}$, as well as the estimation error vectors, $\mathbf{e}_h$ and $\mathbf{e}_g$, we can obtain

$$\tilde{\mathbf{h}}_j = \hat{\tilde{\mathbf{h}}}_j + \tilde{\mathbf{e}}_{h,j}, \text{and } \tilde{\mathbf{g}}_j = \hat{\tilde{\mathbf{g}}}_j + \tilde{\mathbf{e}}_{g,j}, \ (j = 1, 2). \tag{3.19}$$

Then we substitute (3.19) into (3.9), the received SNR at source A under imperfect channel condition γ_A^{rob} in terms of channel estimates and estimation errors can be determined. After ignoring the second-order terms and cross-product of channel estimation errors, both the numerator and denominator of γ_A^{rob} are given by

$$\begin{aligned} r_A^{rob} \approx\ & \mathrm{tr}\left(\mathbf{w}_L \mathbf{w}_L^H \mathbf{a}^H \mathbf{a}\right) + \mathrm{tr}\left(\mathbf{w}_L \mathbf{w}_L^H \left(\mathbf{a}^H \left(\hat{\tilde{\mathbf{g}}}_1 \odot \tilde{\mathbf{e}}_{h,2}\right) + \left(\hat{\tilde{\mathbf{g}}}_1 \odot \tilde{\mathbf{e}}_{h,2}\right)^H \mathbf{a}\right)\right) \\ & + \mathrm{tr}\left(\mathbf{w}_L \mathbf{w}_L^H \left(\mathbf{a}^H \left(\hat{\tilde{\mathbf{h}}}_2 \odot \tilde{\mathbf{e}}_{g,1}\right) + \left(\hat{\tilde{\mathbf{h}}}_2 \odot \tilde{\mathbf{e}}_{g,1}\right)^H\right) \mathbf{a}\right), \end{aligned} \tag{3.20a}$$

$$\begin{aligned} s_A^{rob} =\ & t_n^{\text{rob}} + t_s^{\text{rob}} = t_n^{\text{rob}} \\ \approx\ & \text{tr}\left(\mathbf{w}_L\mathbf{w}_L^H\left(\mathbf{N}^r \odot \left(\hat{\tilde{\mathbf{h}}}_2^H\hat{\tilde{\mathbf{h}}}_2\right)\right)\right) + \text{tr}\left(\mathbf{w}_L\mathbf{w}_L^H\left(\mathbf{N}^r \odot \left(\hat{\tilde{\mathbf{h}}}_2^H\tilde{\mathbf{e}}_{h,2}\right)\right)\right) \\ & + \text{tr}\left(\mathbf{w}_L\mathbf{w}_L^H\left(\mathbf{N}^r \odot \left(\tilde{\mathbf{e}}_{h,2}^H\hat{\tilde{\mathbf{h}}}_2\right)\right)\right), \end{aligned} \tag{3.20b}$$

respectively, where $\mathbf{a} = \hat{\tilde{\mathbf{g}}}_1 \odot \hat{\tilde{\mathbf{h}}}_2$ and $t_s^{\text{rob}} = 0$. Note that though the imperfect self-interference is considered in our initial motivation, the introduced interference resulting from imperfect self-interference cancellation turns out insignificant and negligible[1].

It can be easily shown that the following relations hold true:

$$\mathbf{w}_L\mathbf{w}_L^H\left(\mathbf{x}\odot\mathbf{y}\right)\left(\mathbf{x}\odot\mathbf{z}\right)^H = \mathbf{z}\left(\left(\mathbf{x}\mathbf{x}\right)^T \odot \mathbf{w}_L\mathbf{w}_L^H\right)\mathbf{y}, \tag{3.21a}$$

$$\text{tr}\left(\mathbf{w}_L\mathbf{w}_L^H\left(\left(\mathbf{x}^H\mathbf{y}\right)\odot\mathbf{Z}\right)\right) = \mathbf{y}\left(\mathbf{Z}^T \odot \mathbf{w}_L\mathbf{w}_L^H\right)\mathbf{x}^H, \tag{3.21b}$$

where $\mathbf{x}, \mathbf{y}, \mathbf{z} \in \mathcal{C}^{1\times N^2}$, and $\mathbf{Z} \in \mathcal{C}^{N^2\times N^2}$. By using (3.21a) and (3.21b), and noting that $\mathcal{R}\left\{\mathbf{w}_L^H\mathbf{Z}\mathbf{w}_L\right\} = \mathcal{R}\left\{\mathbf{w}_L^H\mathbf{Z}^H\mathbf{w}_L\right\}$ and $\mathcal{I}\left\{\mathbf{w}_L^H\mathbf{Z}\mathbf{w}_L\right\} = -\mathcal{I}\left\{\mathbf{w}_L^H\mathbf{Z}^H\mathbf{w}_L\right\}$, r_A^{rob} and s_A^{rob} can be simplified to

$$\begin{aligned} r_A^{rob} \approx\ & \text{tr}\left(\mathbf{w}_L\mathbf{w}_L^H\mathbf{a}^H\mathbf{a}\right) + 2\mathcal{R}\left\{\tilde{\mathbf{e}}_{h,2}\left(\left(\hat{\tilde{\mathbf{g}}}_1^H\hat{\tilde{\mathbf{g}}}_1\right)^T \odot \mathbf{w}_L\mathbf{w}_L^H\right)\hat{\tilde{\mathbf{h}}}_2^H\right\} \\ & + 2\mathcal{R}\left\{\tilde{\mathbf{e}}_{g,1}\left(\left(\hat{\tilde{\mathbf{h}}}_2^H\hat{\tilde{\mathbf{h}}}_2\right)^T \odot \mathbf{w}_L\mathbf{w}_L^H\right)\hat{\tilde{\mathbf{g}}}_1^H\right\}, \end{aligned} \tag{3.22a}$$

$$s_A^{rob} \approx \text{tr}\left(\mathbf{w}_L\mathbf{w}_L^H\left(\mathbf{N}^r \odot \left(\hat{\tilde{\mathbf{h}}}_2^H\hat{\tilde{\mathbf{h}}}_2\right)\right)\right) + 2\mathcal{R}\left\{\tilde{\mathbf{e}}_{h,2}\left(\left(\mathbf{N}^r\right)^T \odot \mathbf{w}_L\mathbf{w}_L^H\right)\hat{\tilde{\mathbf{h}}}_2\right\} + \sigma_{n_A}^2. \tag{3.22b}$$

For the transmit power at the MIMO relay, the channel uncertainty should also

[1]In the simulations, the actual received SNR at the sources is calculated including the second-order terms of estimation errors and their cross-product.

be included by incorporating $\mathbf{E}_{UL} = [\mathbf{e}_h \ \mathbf{e}_g]$ into (3.11) as

$$\begin{aligned} P_R^{\text{rob}} &= \mathbf{w}_L^H \hat{\mathbf{C}} \mathbf{w}_L + \text{tr}\left(\mathbf{W}\left(\mathbf{E}_{UL}\hat{\mathbf{H}}_{UL}^H + \hat{\mathbf{H}}_{UL}\mathbf{E}_{UL}^H\right)\mathbf{W}^H\right) \\ &\approx \mathbf{w}_L^H \hat{\mathbf{C}} \mathbf{w}_L + 2\mathcal{R}\left\{\left(\hat{\tilde{\mathbf{h}}}_1 \odot \text{vec}\left(\mathbf{W}^H\mathbf{W}\right)^T\right)\tilde{\mathbf{e}}_{h,2}^H + \left(\hat{\tilde{\mathbf{g}}}_1 \odot \text{vec}\left(\mathbf{W}^H\mathbf{W}\right)^T\right)\tilde{\mathbf{e}}_{g,2}^H\right\}, \end{aligned} \tag{3.23}$$

where $\hat{\mathbf{C}} = \left(\left(\hat{\mathbf{H}}_{UL}\hat{\mathbf{H}}_{UL}^H + \sigma_{n_R}^2\mathbf{I}_N\right)^T \otimes \mathbf{I}_N\right)$.

3.3 Proposed Robust MIMO Relay Design

Typically, robust techniques employ stochastic or worst-case approaches depending upon different CSI error models [41]. The statistics of the CSI error are known under the stochastic philosophy, while the channel error is specified in some uncertainty region in the worst-case method. Since the CSI errors are assumed to be inside the sets of $\mathcal{R}_h$ and $\mathcal{R}_g$ in (3.17), the worst-case approach is exploited in this section to design the robust MIMO relay precoder by optimizing the worst-case performance.

3.3.1 Problem Formulation with Imperfect CSI

The objective of the proposed robust MIMO relay design is to minimize the worst-case transmit power while fulfilling the worst-case SNR constraints at both sources. The so-called worst-case is based upon the largest possible errors $\mathbf{e}_h$ and $\mathbf{e}_g$ which are norm-bounded by δ_h and δ_g, respectively. Hence, the worst-case SNR for each source is the minimum SNR above the predetermined threshold to guarantee the QoS in the presence of largest possible errors. Similarly, the worst-case transmit power is also defined for the largest possible CSI esitmation errors as the maximum power that the MIMO relay needs to forward the linearly processed signal.

Let P_R^{wc} denote the worst-case transmit power whereas γ_A^{wc} denote the worst-case SNR at source A. So P_R^{wc} can be mathematically expressed as

$$P_R^{\text{wc}} = \max_{\|\mathbf{e}_h\| \le \delta_h, \|\mathbf{e}_g\| \le \delta_g} P_R^{\text{rob}}, \tag{3.24}$$

where P_R^{rob} is given by (3.23), and γ_A^{wc} can be written as

$$\gamma_A^{\text{wc}} = \min_{\|\mathbf{e}_h\| \le \delta_h, \|\mathbf{e}_g\| \le \delta_g} \gamma_A^{\text{rob}}. \tag{3.25}$$

Then we modify both the objective of transmit power as well as the QoS conditions in (3.13) by replacing both with the worst-case transmit power of (3.24) and the worst-case received SNR of (3.25) to incorporate the robustness against unknown but norm-bounded channel estimation errors. The so-called robust design of MIMO relay precoder under the worst-case philosophy becomes

$$\begin{aligned} \mathcal{P}^{rob} : & \min_{\mathbf{w}_L} \max_{\|\mathbf{e}_h\| \le \delta_h, \|\mathbf{e}_g\| \le \delta_g} P_R^{\text{rob}} \\ \text{s.t.} \quad & \min_{\|\mathbf{e}_h\| \le \delta_h, \|\mathbf{e}_g\| \le \delta_g} \gamma_k^{\text{rob}} \ge \gamma_{th}, \ k \in \{A, B\}. \end{aligned} \tag{3.26}$$

Note that the objective turns out to minimize the maximum MIMO relay transmit power with respect to the largest possible CSI errors.

Unfortunately, the numerator and denominator of γ_A^{rob}, i.e., (3.22a) and (3.22b) are not independent, which complicates further solving (3.26) to obtain any tractable design. So we strengthen the worst-case QoS constraints by replacing the worst-case received SNR of (3.25) with its lower bound $\tilde{\gamma}_A^{\text{wc}}$ as [50]

$$\gamma_A^{\text{wc}} \ge \frac{\min_{\|\mathbf{e}_h\| \le \delta_h, \|\mathbf{e}_g\| \le \delta_g} r_A^{\text{rob}}}{\max_{\|\mathbf{e}_h\| \le \delta_h} s_A^{\text{rob}}} \triangleq \tilde{\gamma}_A^{\text{wc}}. \tag{3.27}$$

To this end, the proposed optimization problem can be rewritten as

$$\begin{aligned} \mathcal{P} : & \min_{\mathbf{w}_L} P_R^{\text{wc}} \\ \text{s.t.} \ & \tilde{\gamma}_k^{\text{wc}} \ge \gamma_{th}, \ k \in \{A, B\}, \end{aligned} \tag{3.28}$$

where the worst-case SNR is substituted by its lower bound $\tilde{\gamma}_k^{\text{wc}}$.

Moreover, considering the numerator of $\tilde{\gamma}_A^{\text{wc}}$ in (3.27), it's a minimization problem with the estimation errors bounded by their Euclidean norms. Referring to (3.22a), since $\tilde{\mathbf{e}}_{h,2}$ and $\tilde{\mathbf{e}}_{g,1}$ are defined from (3.6) and equal to $\mathbf{e}_h^T \mathbf{D}_2$ and $\mathbf{e}_g^T \mathbf{D}_1$ respectively, we can apply Cauchy-Schwarz inequality to the last two terms of r_A^{rob} and determine

the minimum as

$$\begin{aligned}\min_{\|\mathbf{e}_h\|\leq\delta_h,\|\mathbf{e}_g\|\leq\delta_g} r_A^{\text{rob}} = \text{tr}\left(\mathbf{w}_L\mathbf{w}_L^H\mathbf{a}^H\mathbf{a}\right) - 2\delta_h\left\|\mathbf{D}_2\left(\left(\hat{\tilde{\mathbf{g}}}_1^H\hat{\tilde{\mathbf{g}}}_1\right)^T\odot\mathbf{w}_L\mathbf{w}_L^H\right)\hat{\tilde{\mathbf{h}}}_2^H\right\| \\ - 2\delta_g\left\|\mathbf{D}_1\left(\left(\hat{\tilde{\mathbf{h}}}_2^H\hat{\tilde{\mathbf{h}}}_2\right)^T\odot\mathbf{w}_L\mathbf{w}_L^H\right)\hat{\tilde{\mathbf{g}}}_1^H\right\|.\end{aligned} \tag{3.29}$$

Similarly, the maximization problem of the denominator in (3.27) can also be solved by replacing $\tilde{\mathbf{e}}_{h,2}$ with $\mathbf{e}_h^T\mathbf{D}_2$ and then applying Cauchy-Schwarz inequality to the second term. However, the solution is positive for maximization whereas negative for minimization. So we get

$$\begin{aligned}\max_{\|\mathbf{e}_h\|\leq\delta_h} s_A^{\text{rob}} = \text{tr}\left(\mathbf{w}_L\mathbf{w}_L^H\left(\mathbf{N}^r\odot\left(\hat{\tilde{\mathbf{h}}}_2^H\hat{\tilde{\mathbf{h}}}_2\right)\right)\right) \\ + 2\delta_h\left\|\mathbf{D}_2\left(\left(\mathbf{N}^r\right)^T\odot\mathbf{w}_L\mathbf{w}_L^H\right)\hat{\tilde{\mathbf{h}}}_2^H\right\| + \sigma_{n_A}^2.\end{aligned} \tag{3.30}$$

Applying (3.29) and (3.30) to (3.27), the robust SNR constraint at source A in (3.28) can be given in tractable form. For the problem of maximizing the robust transmit power at the MIMO relay P_R^{rob} as given in (3.24), the worst-case transmit power can be derived as

$$\begin{aligned}\max_{\|\mathbf{e}_h\|\leq\delta_h,\|\mathbf{e}_g\|\leq\delta_g} P_R^{\text{rob}} &= \mathbf{w}_L^H\hat{\mathbf{C}}\mathbf{w}_L + 2\delta_h\left\|\mathbf{D}_2\left(\hat{\tilde{\mathbf{h}}}_1\odot\text{vec}\left(\mathbf{W}^H\mathbf{W}\right)^T\right)\right\| \\ &\quad + 2\delta_g\left\|\mathbf{D}_2\left(\hat{\tilde{\mathbf{g}}}_1\odot\text{vec}\left(\mathbf{W}^H\mathbf{W}\right)^T\right)\right\| \\ &\triangleq \mathbf{w}_L^H\hat{\mathbf{C}}\mathbf{w}_L + 2\delta_h\left\|\mathbf{H}_A\text{vec}\left(\mathbf{w}_L\mathbf{w}_L^H\right)\right\| + 2\delta_g\left\|\mathbf{H}_B\text{vec}\left(\mathbf{w}_L\mathbf{w}_L^H\right)\right\|,\end{aligned} \tag{3.31}$$

where $\mathbf{H}_A, \mathbf{H}_B \in \mathcal{C}^{N\times N^4}$ can be constructed by using the pseudocode presented in Table 3.1.

The same approach can be applied to the transmission from A to B to derive the robust SNR constraint at source B. Finally, the proposed optimization problem in

Table 3.1: Pesudocode for constructing $\mathbf{H}_A$ and $\mathbf{H}_B$.

Step 1:	Initialization: $l = 0, \tilde{\mathbf{H}}_A = \tilde{\mathbf{H}}_B = \text{zeros}(N^2, N^4)$.
Step 2:	For $j = 1 : N$
Step 3:	For $i = 1 : N$
Step 4:	$l = l + 1$;
	$p = [(i-1)N^3 + (j-1)N + 1 : N^2 + 1 : iN^3 + jN]$;
	$\tilde{\mathbf{H}}_A(l, p) = \hat{\mathbf{h}}_1(l)$, $\tilde{\mathbf{H}}_B(l, p) = \hat{\mathbf{g}}_1(l)$
Step 5:	End Step 3.
Step 6:	End Step 2.
Step 7:	$\mathbf{H}_A = \mathbf{D}_2\tilde{\mathbf{H}}_A$, $\mathbf{H}_B = \mathbf{D}_2\tilde{\mathbf{H}}_B$, where $\mathbf{D}_2 = \mathbf{1}_{1\times N} \otimes \mathbf{I}_N$ as provided in (3.6).

(3.28) can be specified as

$$
\begin{aligned}
&\mathcal{P} : \min_{\mathbf{w}_L} \mathbf{w}_L^H \hat{\mathbf{C}} \mathbf{w}_L + 2\delta_h \left\| \mathbf{H}_A \text{vec}\left(\mathbf{w}_L \mathbf{w}_L^H\right) \right\| + 2\delta_g \left\| \mathbf{H}_B \text{vec}\left(\mathbf{w}_L \mathbf{w}_L^H\right) \right\| \\
&\text{s.t. } \text{tr}\left(\mathbf{w}_L \mathbf{w}_L^H \left(\mathbf{a}^H \mathbf{a} - \gamma_{th}\left(\mathbf{N}^r \odot \left(\hat{\hat{\mathbf{h}}}_2^H \hat{\hat{\mathbf{h}}}_2\right)\right)\right)\right) \\
&\geq 2\delta_h \left\| \mathbf{D}_2 \left(\left(\hat{\hat{\mathbf{g}}}_1^H \hat{\hat{\mathbf{g}}}_1\right)^T \odot \mathbf{w}_L \mathbf{w}_L^H\right) \hat{\hat{\mathbf{h}}}_2^H \right\| + 2\delta_g \left\| \mathbf{D}_1 \left(\left(\hat{\hat{\mathbf{h}}}_2^H \hat{\hat{\mathbf{h}}}_2\right)^T \odot \mathbf{w}_L \mathbf{w}_L^H\right) \hat{\hat{\mathbf{g}}}_1^H \right\| \\
&+ 2\gamma_{th}\delta_h \left\| \mathbf{D}_2 \left(\left(\mathbf{N}^r\right)^T \odot \mathbf{w}_L \mathbf{w}_L^H\right) \hat{\hat{\mathbf{h}}}_2^H \right\| + \gamma_{th}\sigma_{n_A}^2, \\
&\quad \text{tr}\left(\mathbf{w}_L \mathbf{w}_L^H \left(\mathbf{b}^H \mathbf{b} - \gamma_{th}\left(\mathbf{N}^r \odot \left(\hat{\hat{\mathbf{g}}}_2^H \hat{\hat{\mathbf{g}}}_2\right)\right)\right)\right) \\
&\geq 2\delta_g \left\| \mathbf{D}_2 \left(\left(\hat{\hat{\mathbf{h}}}_1^H \hat{\hat{\mathbf{h}}}_1\right)^T \odot \mathbf{w}_L \mathbf{w}_L^H\right) \hat{\hat{\mathbf{g}}}_2^H \right\| + 2\delta_h \left\| \mathbf{D}_1 \left(\left(\hat{\hat{\mathbf{g}}}_2^H \hat{\hat{\mathbf{g}}}_2\right)^T \odot \mathbf{w}_L \mathbf{w}_L^H\right) \hat{\hat{\mathbf{h}}}_1^H \right\| \\
&+ 2\gamma_{th}\delta_g \left\| \mathbf{D}_2 \left(\left(\mathbf{N}^r\right)^T \odot \mathbf{w}_L \mathbf{w}_L^H\right) \hat{\hat{\mathbf{g}}}_2^H \right\| + \gamma_{th}\sigma_{n_B}^2,
\end{aligned}
\tag{3.32}
$$

where $\mathbf{a} = \hat{\hat{\mathbf{g}}}_1 \odot \hat{\hat{\mathbf{h}}}_2$ and $\mathbf{b} = \hat{\hat{\mathbf{h}}}_1 \odot \hat{\hat{\mathbf{g}}}_2$.

3.3.2 Semidefinite Relaxation based Approximation

By observing the optimization problem of (3.32), both the objective and constraints consist of the second-order terms of $\mathbf{w}_L$ inside the norms and accordingly are non-convex. However, after some tricky manipulation step by step, this problem can be solved, and an approximate solution to $\mathcal{P}$ can be obtained. We refer to this approach as the two-stage SDR-based approximation [46].

Define $\tilde{\mathbf{W}} = \mathbf{w}_L \mathbf{w}_L^H \in \mathcal{C}^{MM\times MM}$, then $\tilde{\mathbf{W}} \succeq 0$ and $\text{rank}(\tilde{\mathbf{W}}) = 1$. It can be easily shown that $\mathbf{w}_L^H \mathbf{X} \mathbf{w}_L = \text{tr}(\mathbf{w}_L^H \mathbf{X} \mathbf{w}_L) = \text{tr}(\mathbf{X} \mathbf{w}_L \mathbf{w}_L^H) = \text{tr}(\mathbf{X}\tilde{\mathbf{W}})$. Now we change the

optimization variable in (3.32) from $\mathbf{w}_L$ to $\tilde{\mathbf{W}}$, and rewrite the optimization problem in terms of $\tilde{\mathbf{W}}$ as

$$\begin{aligned}
&\mathcal{P}_2 : \min_{\tilde{\mathbf{W}}} \operatorname{tr}\left(\hat{\mathbf{C}}\tilde{\mathbf{W}}\right) + 2\delta_h \left\|\mathbf{H}_A \operatorname{vec}\left(\tilde{\mathbf{W}}\right)\right\| + 2\delta_g \left\|\mathbf{H}_B \operatorname{vec}\left(\tilde{\mathbf{W}}\right)\right\| \\
&\text{s.t. } \operatorname{tr}\left(\mathbf{A}\tilde{\mathbf{W}}\right) \geq 2\delta_h \left\|\mathbf{D}_2\left(\left(\hat{\tilde{\mathbf{g}}}_1^H \hat{\tilde{\mathbf{g}}}_1\right)^T \odot \tilde{\mathbf{W}}\right)\hat{\tilde{\mathbf{h}}}_2^H\right\| + 2\delta_g \left\|\mathbf{D}_1\left(\left(\hat{\tilde{\mathbf{h}}}_2^H \hat{\tilde{\mathbf{h}}}_2\right)^T \odot \tilde{\mathbf{W}}\right)\hat{\tilde{\mathbf{g}}}_1^H\right\| \\
&+ 2\gamma_{th}\delta_h \left\|\mathbf{D}_2\left(\left(\mathbf{N}^r\right)^T \odot \tilde{\mathbf{W}}\right)\hat{\tilde{\mathbf{h}}}_2^H\right\| + \gamma_{th}\sigma_{n_A}^2, \\
&\quad \operatorname{tr}\left(\mathbf{B}\tilde{\mathbf{W}}\right) \geq 2\delta_g \left\|\mathbf{D}_2\left(\left(\hat{\tilde{\mathbf{h}}}_1^H \hat{\tilde{\mathbf{h}}}_1\right)^T \odot \tilde{\mathbf{W}}\right)\hat{\tilde{\mathbf{g}}}_2^H\right\| + 2\delta_h \left\|\mathbf{D}_1\left(\left(\hat{\tilde{\mathbf{g}}}_2^H \hat{\tilde{\mathbf{g}}}_2\right)^T \odot \tilde{\mathbf{W}}\right)\hat{\tilde{\mathbf{h}}}_1^H\right\| \\
&+ 2\gamma_{th}\delta_g \left\|\mathbf{D}_2\left(\left(\mathbf{N}^r\right)^T \odot \tilde{\mathbf{W}}\right)\hat{\tilde{\mathbf{g}}}_2^H\right\| + \gamma_{th}\sigma_{n_B}^2, \\
&\quad \tilde{\mathbf{W}} \succeq 0, \ \operatorname{rank}(\tilde{\mathbf{W}}) = 1,
\end{aligned} \tag{3.33}$$

where $\mathbf{A} = \mathbf{a}^H\mathbf{a} - \gamma_{th}\left(\mathbf{N}^r \odot \left(\hat{\tilde{\mathbf{h}}}_2^H \hat{\tilde{\mathbf{h}}}_2\right)\right)$ and $\mathbf{B} = \mathbf{b}^H\mathbf{b} - \gamma_{th}\left(\mathbf{N}^r \odot \left(\hat{\tilde{\mathbf{g}}}_2^H \hat{\tilde{\mathbf{g}}}_2\right)\right)$.

The problem $\mathcal{P}_2$ is still nonconvex due to the last $\tilde{\mathbf{W}}$ rank-one constraint in (3.33). After removing this nonconvex constraint, we obtain a relaxation counterpart of (3.33) denoted by $\mathcal{P}_3$ as shown below.

$$\begin{aligned}
&\mathcal{P}_3 : \min_{\tilde{\mathbf{W}}} \operatorname{tr}\left(\hat{\mathbf{C}}\tilde{\mathbf{W}}\right) + 2\delta_h \left\|\mathbf{H}_A \operatorname{vec}\left(\tilde{\mathbf{W}}\right)\right\| + 2\delta_g \left\|\mathbf{H}_B \operatorname{vec}\left(\tilde{\mathbf{W}}\right)\right\| \\
&\text{s.t. } \operatorname{tr}\left(\mathbf{A}\tilde{\mathbf{W}}\right) \geq 2\delta_h \left\|\mathbf{D}_2\left(\left(\hat{\tilde{\mathbf{g}}}_1^H \hat{\tilde{\mathbf{g}}}_1\right)^T \odot \tilde{\mathbf{W}}\right)\hat{\tilde{\mathbf{h}}}_2^H\right\| + 2\delta_g \left\|\mathbf{D}_1\left(\left(\hat{\tilde{\mathbf{h}}}_2^H \hat{\tilde{\mathbf{h}}}_2\right)^T \odot \tilde{\mathbf{W}}\right)\hat{\tilde{\mathbf{g}}}_1^H\right\| \\
&+ 2\gamma_{th}\delta_h \left\|\mathbf{D}_2\left(\left(\mathbf{N}^r\right)^T \odot \tilde{\mathbf{W}}\right)\hat{\tilde{\mathbf{h}}}_2^H\right\| + \gamma_{th}\sigma_{n_A}^2, \\
&\quad \operatorname{tr}\left(\mathbf{B}\tilde{\mathbf{W}}\right) \geq 2\delta_g \left\|\mathbf{D}_2\left(\left(\hat{\tilde{\mathbf{h}}}_1^H \hat{\tilde{\mathbf{h}}}_1\right)^T \odot \tilde{\mathbf{W}}\right)\hat{\tilde{\mathbf{g}}}_2^H\right\| + 2\delta_h \left\|\mathbf{D}_1\left(\left(\hat{\tilde{\mathbf{g}}}_2^H \hat{\tilde{\mathbf{g}}}_2\right)^T \odot \tilde{\mathbf{W}}\right)\hat{\tilde{\mathbf{h}}}_1^H\right\| \\
&+ 2\gamma_{th}\delta_g \left\|\mathbf{D}_2\left(\left(\mathbf{N}^r\right)^T \odot \tilde{\mathbf{W}}\right)\hat{\tilde{\mathbf{g}}}_2^H\right\| + \gamma_{th}\sigma_{n_B}^2, \\
&\quad \tilde{\mathbf{W}} \succeq 0,
\end{aligned} \tag{3.34}$$

which is a convex optimization problem. Note that by introducing a new variable, $\mathcal{P}_3$ can be easily reformulated as a standard semidefinite programming (SDP) problem consisting of linear objective and SOC and positive semidefinite constraints. The convex problem of (3.34) can be efficiently solved with Matlab by using the `YALMIP`

toolbox [2] [51, 52].

The optimization problem $\mathcal{P}_3$ subsumes the problem $\mathcal{P}_2$, since the feasible region of $\mathcal{P}_2$ is a subset of that of $\mathcal{P}_3$. In general, the optimal solution to $\mathcal{P}_3$ is of rank r with $r > 1$ rather than rank-one, which makes $\mathcal{P}_2$ infeasible. The Gaussian randomization technique [21, 46, 47, 53] can be adopted to construct a feasible rank-one solution to $\mathcal{P}_2$ from the optimal solution of relaxed SDP problem $\mathcal{P}_3$. So the two-stage SDR-based approximation method used in this chapter consists of solving the relaxation problem $\mathcal{P}_3$ in the first stage and then applying the randomization technique to the optimal solution of $\mathcal{P}_3$ in the second stage. This method will lead to an approximate solution to $\mathcal{P}_2$. In the following, the Gaussian randomization method is presented.

Let $\tilde{\mathbf{W}}^{\text{opt}}$ denote the optimal solution to $\mathcal{P}_3$ in (3.34). The idea behind the Gaussian randomization is to generate a large number of candidate vectors representing the MIMO relay precoder matrix from $\tilde{\mathbf{W}}^{\text{opt}}$ and choose the one that can be scaled to guarantee the SNR constraints of $\mathcal{P}_2$ in (3.33) at the minimum transmit power cost. Initially, the eigenvalue decomposition of the optimal matrix $\tilde{\mathbf{W}}^{\text{opt}}$ is calculated as $\tilde{\mathbf{W}}^{\text{opt}} = \mathbf{U}\mathbf{\Sigma}\mathbf{U}^H$. Let $\mathbf{v}_L$ be a column vector of N^2 zero-mean, unit-variance complex circularly symmetric uncorrelated Gaussian r.v.'s, i.e., $\mathbf{v}_L \sim \mathcal{CN}(0, \mathbf{I}_{N^2})$. Then the candidate vector $\mathbf{w}_L^{\text{c}}$ is constructed as $\mathbf{w}_L^{\text{c}} = \mathbf{U}\mathbf{\Sigma}^{1/2}\mathbf{v}_L$, and the MIMO relay precoder matrix can herein be obtained through the reverse vectorization operation as $\mathbf{W}^{\text{c}} = \text{vec}^{-1}(\mathbf{w}_L^{\text{c}})$. This ensures that $\mathbb{E}[\mathbf{w}_L^{\text{c}}(\mathbf{w}_L^{\text{c}})^H] = \tilde{\mathbf{W}}^{\text{opt}}$, denoted by $\mathbf{w}_L^{\text{c}} \sim \mathcal{CN}(\mathbf{0}, \tilde{\mathbf{W}}^{\text{opt}})$.

Since $\mathbf{w}_L^{\text{c}}$ depends on the particular realization of $\mathbf{v}_L$, the constraints of the original problem $\mathcal{P}$ in (3.32) might be violated or over-satisfied. Accordingly we can seek a positive boost or reduction factor to scale $\mathbf{w}_L^{\text{c}}$ to the minimum length that is necessary to satisfy the constraints. Denote the scale factor as $\sqrt{\lambda}$, and based upon the problem

[2] `YALMIP` is to concentrate on the language and the higher level algorithms, while relying on external solver such as `SeDuMi` for the actual computations [51].

$\mathcal{P}_2$ in (3.33) define

$$\begin{aligned}
\alpha &= \mathrm{tr}\left(\hat{\mathbf{C}}\tilde{\mathbf{W}}^{\mathrm{c}}\right) + 2\delta_h \left\|\mathbf{H}_A \mathrm{vec}\left(\tilde{\mathbf{W}}^{\mathrm{c}}\right)\right\| + 2\delta_g \left\|\mathbf{H}_B \mathrm{vec}\left(\tilde{\mathbf{W}}^{\mathrm{c}}\right)\right\|, \\
\beta_A &= \mathrm{tr}\left(\mathbf{A}\tilde{\mathbf{W}}^{\mathrm{c}}\right) - 2\delta_h \left\|\mathbf{D}_2\left(\left(\hat{\tilde{\mathbf{g}}}_1^H \hat{\tilde{\mathbf{g}}}_1\right)^T \odot \tilde{\mathbf{W}}^{\mathrm{c}}\right)\hat{\tilde{\mathbf{h}}}_2^H\right\| \\
&\quad - 2\delta_g \left\|\mathbf{D}_1\left(\left(\hat{\tilde{\mathbf{h}}}_2^H \hat{\tilde{\mathbf{h}}}_2\right)^T \odot \tilde{\mathbf{W}}^{\mathrm{c}}\right)\hat{\tilde{\mathbf{g}}}_1^H\right\| - 2\gamma_{th}\delta_h \left\|\mathbf{D}_2\left(\left(\mathbf{N}^r\right)^T \odot \tilde{\mathbf{W}}^{\mathrm{c}}\right)\hat{\tilde{\mathbf{h}}}_2^H\right\|, \qquad (3.35) \\
\beta_B &= \mathrm{tr}\left(\mathbf{B}\tilde{\mathbf{W}}^{\mathrm{c}}\right) - 2\delta_g \left\|\mathbf{D}_2\left(\left(\hat{\tilde{\mathbf{h}}}_1^H \hat{\tilde{\mathbf{h}}}_1\right)^T \odot \tilde{\mathbf{W}}^{\mathrm{c}}\right)\hat{\tilde{\mathbf{g}}}_2^H\right\| \\
&\quad - 2\delta_h \left\|\mathbf{D}_1\left(\left(\hat{\tilde{\mathbf{g}}}_2^H \hat{\tilde{\mathbf{g}}}_2\right)^T \odot \tilde{\mathbf{W}}^{\mathrm{c}}\right)\hat{\tilde{\mathbf{h}}}_1^H\right\| - 2\gamma_{th}\delta_g \left\|\mathbf{D}_2\left(\left(\mathbf{N}^r\right)^T \odot \tilde{\mathbf{W}}^{\mathrm{c}}\right)\hat{\tilde{\mathbf{g}}}_2^H\right\|,
\end{aligned}$$

where $\tilde{\mathbf{W}}^{\mathrm{c}} = \mathbf{w}_L^{\mathrm{c}}(\mathbf{w}_L^{\mathrm{c}})^H$. Then, it turns out that the following problem can be resorted to converting the candidate MIMO relay precoder to the candidate solution to $\mathcal{P}_2$.

$$\mathcal{Q} : \min_{\lambda \geq 0} \lambda\alpha \text{ s.t. } \lambda\beta_k \geq \gamma_{th}\sigma_{n_k}^2, k \in \{A, B\}. \qquad (3.36)$$

Problem $\mathcal{Q}$ is a linear programming (LP) with a single variable λ and linear inequality constraints. For a feasible instance of the LP problem $\mathcal{Q}$, it is obvious that β_k should be positive. So for those $\mathbf{w}_L^{\mathrm{c}}$ candidates that make β_k positive, the scaling factor can be easily solved as

$$\lambda = \max\left(\frac{\gamma_{th}\sigma_{n_A}^2}{\beta_A}, \frac{\gamma_{th}\sigma_{n_B}^2}{\beta_B}\right). \qquad (3.37)$$

Therefore, the two-stage SDR-based approximation algorithm for generating an approximate solution to the original problem $\mathcal{P}$ can be summarized as

- **Relaxation**: Solve the relaxed equivalent SDP problem $\mathcal{P}_3$ and obtain the optimal solution $\tilde{\mathbf{W}}^{\mathrm{opt}}$.
- **Randomization**: Check the rank of $\tilde{\mathbf{W}}^{\mathrm{opt}}$.
  - If $\tilde{\mathbf{W}}^{\mathrm{opt}} = 1$, then use its principal eigenvector as the optimal solution to problem $\mathcal{P}$.
  - Otherwise, generate a candidate $\mathbf{w}_L^{\mathrm{c}}$ by using the aforementioned Gaussian randomization method. Calculate $\beta_k, k \in \{A, B\}$ in (3.35), and if negative discard the corresponding candidate $\mathbf{w}_L^{\mathrm{c}}$. Otherwise, determine and record the scaling factor λ from (3.37), as well as the associated objective

value in (3.36) and the candidate vector. Repeat a large enough number[3] of the randomization procedures. In the end, choose the candidate and scaling factor with the minimum objective value, denoted by $\mathbf{w}_L^\circ$ and λ°, respectively.

The approximated optimal solution to problem $\mathcal{P}$ can be given as $\mathbf{w}_L^{\text{opt}} = \sqrt{\lambda^\circ}\mathbf{w}_L^\circ$. The robust MIMO relay precoder matrix can herein be determined through the reverse vectorization operation as $\mathbf{W}^{\text{opt}} = \text{vec}^{-1}(\mathbf{w}_L^{\text{opt}})$.

3.4 Numerical Results and Discussion

This section will first provides a numerical example to show the robustness capabilities of the presented design and compare its performance with the nonrobust approach [17]. In this example, we take $N = 3$, and consider the standard i.i.d. Rayleigh fading model – the elements of each channel vector between the source and relay are i.i.d. CGRV with zero-mean and unit variance. For all simulations, the channel estimates are given as $\hat{\mathbf{h}} = [0.6282 - 0.8111i \quad -2.0819 + 1.0171i \quad 0.9689 - 1.2102i]^T$ and $\hat{\mathbf{g}} = [-0.7558 - 0.5724i \quad 0.2299 - 0.5338i \quad -0.0723 - 0.1707i]^T$, and the noise power at the MIMO relay and sources are fixed at -20 and 0 dBW respectively. Furthermore, we assume that the error variances are identical across all links, i.e., $\sigma_{e_{h_i}}^2 = \sigma_{e_{g_i}}^2 = \sigma_e^2$ or $\delta_h = \delta_g = \delta$. Through Fig. 3.2 to 3.5, we take the error variance $\sigma_e^2 = 0.002$, and the upper norm-bound δ_h can be calculated by using a numerical search based on (3.18). The optimization problem $\mathcal{P}_3$ in (3.34) is solved using the `YALMIP` toolbox[4]. If the solution matrix $\tilde{\mathbf{W}}^{\text{opt}}$ turns out being rank one, the associated principal component solves the original problem $\mathcal{P}$. Otherwise, the SDR-based approximation in Sec. 3.3.2 is carried out. With the obtained optimal $\mathbf{w}_L$, the worst-case transmit power at the MIMO relay is calculated based on (3.31). Moreover, after substituting $\mathbf{H}_{UL} = \hat{\mathbf{H}}_{UL} + \mathbf{E}_{UL}$ into (3.11) and then averaging over 1,000 independent realizations of estimation errors $\mathbf{e}_h$ and $\mathbf{e}_g$, the average transmit power of the robust method is obtained. For comparing purpose, the nonrobust method in (3.13) is implemented to obtain the optimal solution denoted by $\mathbf{w}_L^{nrob}$

[3] In our numerical results, we run the randomization loop till generating 1,000 candidates with positive $\beta_k, k \in \{A, B\}$ in (3.35).

[4] Since $\mathcal{P}_3$ is essentially a SDP problem, and can be efficiently solved using interior point method, at a complexity cost that is at most $O((M + N^2)^{3.5})$ and is usually much less [47]. In all of our simulations, `YALMIP` takes seconds to solve $\mathcal{P}_3$ if a feasible solution exists.

without taking into account the channel estimation error. Similarly, the transmit power for the nonrobust method with $\mathbf{w}_L^{nrob}$ in (3.11) is averaged by considering 1,000 random realizations of $\mathbf{e}_h$ and $\mathbf{e}_g$.

Fig. 3.2 illustrates the transmit power at the MIMO relay versus SNR threshold γ_{th} for both robust and nonrobust methods. Denote $\eta = \Pr\{\sigma_{e_h}^2 T \leq \delta_h^2\}$, and $1-\eta$ is fixed at 0.12 in this figure which corresponds to δ of 0.108. As shown in Fig. 3.2, the transmit power increases for all cases with the increasing γ_{th}. It is intuitive to expect that the MIMO relay requires more power in order to guarantee higher QoS requirement at the sources. For the robust method, the worst-case transmit power is larger than the average power, which can also be observed from that (3.31) has two more terms comparing to (3.11). Moreover, the average transmit power curve of the nonrobust method lies below that of the robust method as expected, since more power is needed to combat channel uncetainty. The power gap between robust and nonrobust methods is around 2 dBW, and what kind of performance increase can this extra cost bring? To answer this question, we plot the outage probability for each source in Fig. 3.3 as a function of SNR threshold based on the same simulation parameters of Fig. 3.2. It should be noted that the outage probability here is not the conventionally defined one to indicate the fading of the channel itself, but refer to the probability that the received SNR at the sources is below the threshold for the given channel estimates due to the CSI errors. The actual received SNR in the simulations is calculated for both sources including the second-order terms of estimation errors. The outage probability is averaged over 1,000 independent trials, and in each trial 1,000 outage events are captured by randomly generating the estimation errors. It can be observed from Fig. 3.3 that both sources have almost the same outage probability resulting from the symmetric channel condition. Furthermore, the outage probability for the nonrobust method is affected deeply by the channel estimation errors, whereas the proposed robust mehthod efficiently combats the effect of estimation errors as the outage probability remains zero-outage through all the SNR range.

Next, Figs. 3.4 and 3.5 investigate the outage probability for the robust and nonrobust methods under the same amount of average transmit power. Take the average transmit power of the nonrobust method in Fig. 3.2 as a baseline, the appropriate η or δ in the robust method is determined with the help of numerical search for each SNR threshold to achieve almost the same average transmit power at the relay as in the nonrobust method. The resulting average transmit power is plotted in Fig. 3.4. As shown in Fig. 3.5, the outage probability of each source for the robust method is

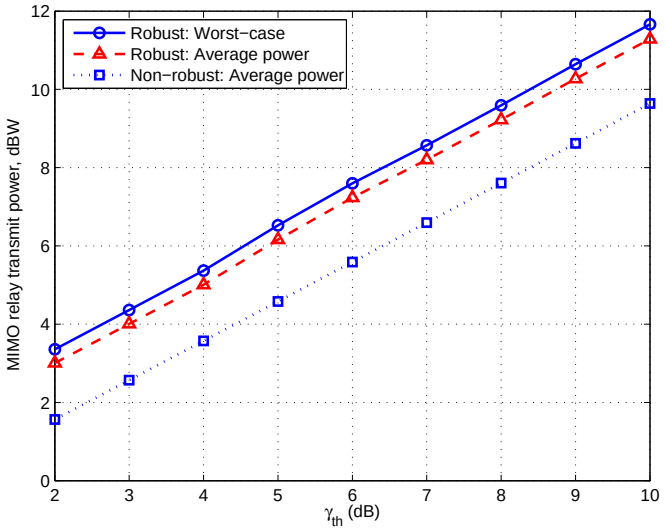

Figure 3.2: Transmit power at the MIMO relay versus received SNR threshold γ_{th} for the robust $(1-\eta = 0.12)$ and nonrobust methods. σ_e^2 is fixed at 0.002.

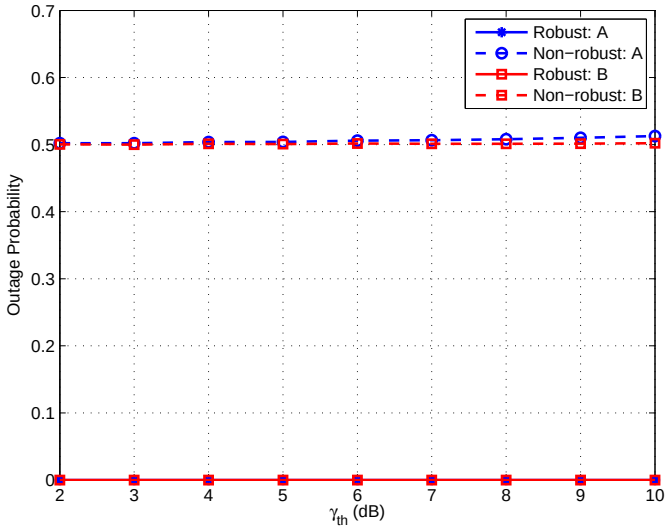

Figure 3.3: Outage probability of SNR versus received SNR threshold γ_{th} at both sources for the robust $(1-\eta = 0.12)$ and nonrobust methods. σ_e^2 is fixed at 0.002.

still zero, fully exhibiting the robustness of the proposed MIMO relay design against the influence of estimation errors. So we can conclude that the robust method far outperforms the nonrobust method in terms of outage probability with the same or similar average transmit powers at the MIMO relay.

In Fig. 3.6 and 3.7, we plot the transmit power at the MIMO relay and the outage probability of SNR for both sources versus the error variance σ_e^2, respectively. We take $1-\eta = 0.12$ and $\gamma_{th} = 8$ dB for both figures. It can be observed from Fig. 3.6 that the average transmit power remains almost the same across different CSI errors for both the robust and nonrobust method, and the robust method needs more transmit power to provide the robustness against the channel uncertianty than the nonrobust method. As before, the outage probability of SNR versus σ_e^2 in the given range remains zero for the robust method whereas more than 50% for the nonrobust method. So the proposed robust method can serve the QoS requirement for both sources but at the cost of a larger transmit power at the MIMO relay.

Besides the performance improvement, the feasibility issue is also of interest. Since problem $\mathcal{P}_3$ is a relaxation of problem $\mathcal{P}_2$, if $\mathcal{P}_2$ is feasible so is $\mathcal{P}_3$. But the converse is generally not true – if $\mathcal{P}_3$ is feasible, $\mathcal{P}_2$ is not necessarily feasible. In order to establish the feasibility of the proposed two-stage SDR-based approximation, the first is that $\mathcal{P}_3$ is feasible, and once a feasible solution to $\mathcal{P}_3$ is found the randomization loop should yield at least one feasible solution, i.e., $\beta_k, k \in \{A, B\}$ in (3.35) should be positive. It has been verified in the simulations that if the randomization loop can yield at least one feasible solution, each randomization procedure of the loop can give a feasible solution. So after a large number of randomization procedures to generate a predetermined number[5] of feasible solutions, the best feasible solution can be selected as the approximated optimum solution to the original problem $\mathcal{P}$. This is most often the case. Otherwise, the randomization loop will fail to return any feasible solution. Note that the randomization loop is another factor contributing to the complexity of the SDR-based approximation algorithm. As long as the randomization loop can yield at least one feasible solution, the randomization loop will run a predetermined number of times and each run will generate a feasible solution. So the complexity of the randomization loop is $O(1)$ under the condition that the feasible solution exists. In our simulations, it usually takes around one second to generate 1,000 candidates based on 2.4 GHz Intel Core 2 Duo processor. So plus the time solving the relaxed optimization problem $\mathcal{P}_3$, the total processing time to yield an optimal approximate solution to

[5]In our simulations, we choose 1,000.

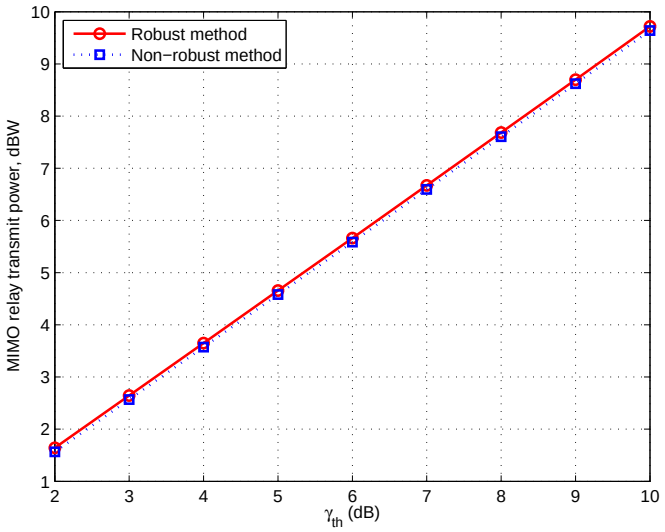

Figure 3.4: Transmit power at the MIMO relay versus received SNR threshold γ_{th} for the robust ($1-\eta$ is adjusted for each γ_{th}) and nonrobust methods. σ_e^2 is fixed at 0.002.

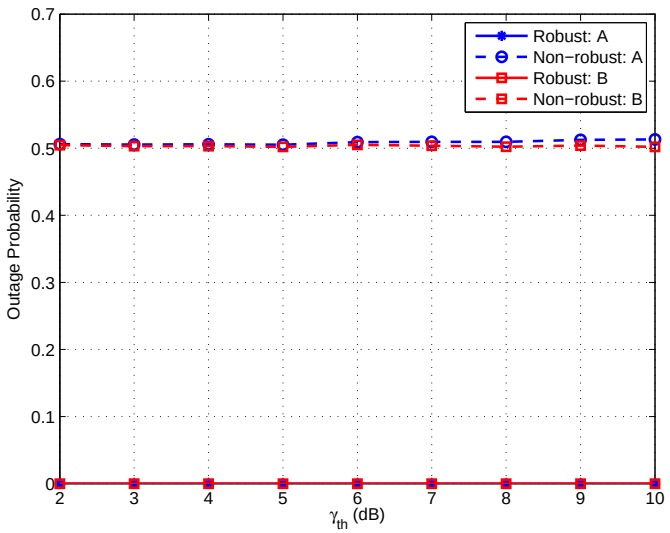

Figure 3.5: Outage probability of SNR versus received SNR threshold γ_{th} at both sources for the robust ($1-\eta$ is adjusted for each γ_{th}) and nonrobust methods. σ_e^2 is fixed at 0.002.

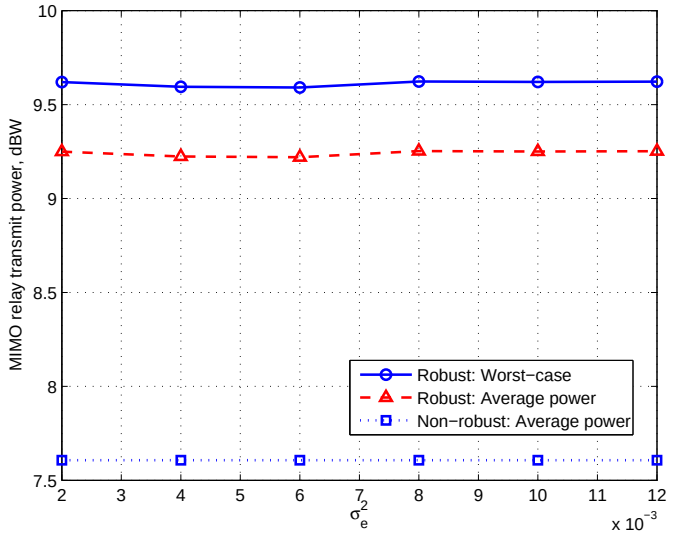

Figure 3.6: Transmit power at the MIMO relay versus error variance σ_e^2 for the robust $(1-\eta = 0.12)$ and nonrobust methods. γ_{th} is fixed at 8 dB.

the original problem $\mathcal{P}$ is in the time order of seconds. It can also be concluded that the feasibility issue is of more significance than the algorithm complexity.

Feasibility depends on various factors: namely, the number of transmit antennas, the channel characteristics, the noise variance, and finally the received SNR threshold, which will be investigated in the simulations by exploiting 1,000 different channel realizations. For each simulation run, the feasibility of $\mathcal{P}_3$ is first verified. If $\mathcal{P}_3$ is feasible, the randomization loop will be carried out to see if any feasible $\mathbf{w}_L$ to the original problem $\mathcal{P}$ can be yielded. Table 3.2 compares different number of transmit antennas, i.e., $N = 3$ and $N = 6$ with fixed noise variance of 0.1 at the MIMO relay, while Table 3.3 fixes the number of transmit antennas at $N = 3$ and compares the different noise variance of 1 and 0.01. For each such configuration, the same received SNR targets are requested for both sources ranging from 2 dB to 14 dB, so the impact of received SNR threshold is also investigated. The other simulation parameters are the same as aforementioned.

The number of 1,000 simulations and corresponding percentage for which $\mathbf{P}_3$ is feasible are listed in the columns "Feas. $\mathcal{P}_3$", in which "#" denotes the number and "%" represents the percentage. Columns "Feas. appr." report the number of problem instances (in terms of 1,000 simulations) for which, once a feasible solution

Table 3.2: Simulation results with various transmit antennas $N = 3$ and $N = 6$ versus received SNR threshold based on 1,000 different independent channel realizations. The noise variance at the MIMO relay N_r is fixed at 0.1.

γ_{th}	$N = 3$				$N = 6$			
	Feas. $\mathcal{P}_3$		Feas. appr.		Feas. $\mathcal{P}_3$		Feas. appr.	
	#	%	#	%	#	%	#	%
2	974	97.4	965	99.1	995	99.5	995	100
4	950	95.0	932	98.1	991	99.1	991	100
6	899	89.9	870	96.8	971	97.1	970	99.9
8	795	79.5	752	94.6	927	92.7	922	99.5
10	597	59.7	513	85.9	831	83.1	808	97.2
12	341	34.1	262	76.8	672	67.2	596	88.7
14	93	9.3	70	75.3	339	33.9	277	81.7

Table 3.3: Simulation results with various noise variance $N_r = 0.1$ and $N_r = 0.01$ versus received SNR threshold based on 1,000 different independent channel realizations. The number of transmit antennas at MIMO relay N is fixed at 3.

γ_{th}	$N_r = 1$				$N_r = 0.01$			
	Feas. $\mathcal{P}_3$		Feas. appr.		Feas. $\mathcal{P}_3$		Feas. appr.	
	#	%	#	%	#	%	#	%
2	341	34.1	273	80.6	995	99.5	993	99.8
4	93	9.3	71	76.3	995	99.5	990	99.5
6	14	1.4	10	71.4	994	99.4	988	99.4
8	1	0.1	-	-	988	98.8	980	99.2
10	-	-	-	-	984	98.4	976	99.2
12	-	-	-	-	972	97.2	962	99.0
14	-	-	-	-	948	94.8	929	98.0

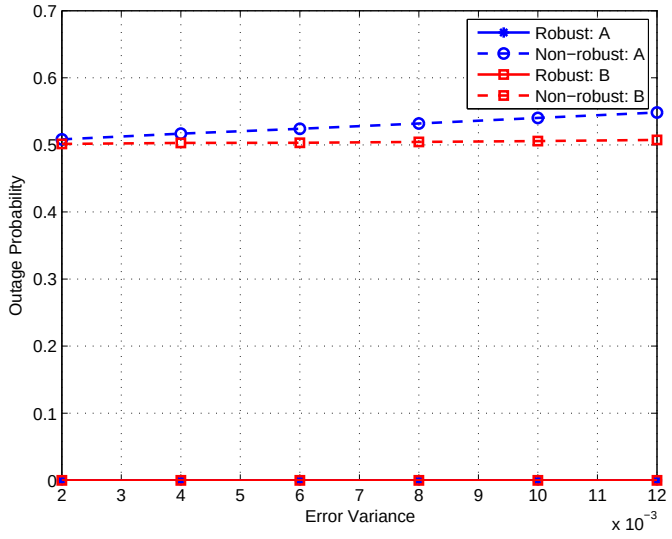

Figure 3.7: Outage probability of SNR versus error variance σ_e^2 at both sources for the robust $(1-\eta = 0.12)$ and nonrobust methods. γ_{th} is fixed at 8 dB.

to $\mathcal{P}_3$ is found, the randomization loop yields at least one feasible solution, as well as the corresponding percentage (in terms of the number of "Feas. $\mathcal{P}_3$"). In all configuration considered, the higher the received SNR threshold, the less likely it is that $\mathcal{P}_3$ is feasible and that the randomization loop yields feasible solution to $\mathcal{P}$. It can be observed in Table 3.2 that increasing the number of transmit antennas at the MIMO relay increases the feasibility for both relaxation and randomization. This observation can be expected since exploring more antennas can better combat the channel uncertainty by providing higher received SNR for both sources. Finally, $\mathcal{P}_3$ is getting more difficult to solve for higher noise variance at the MIMO relay as illustrated in Table 3.3.

3.5 Conclusions

In this chapter, we have addressed the robust MIMO relay design problem in TWRN and provided the robust MIMO relay design based on the channel estimates. The channel estimation error has been explicitly taken into account in the design, and the worst-case philosophy has been adopted to include the robustness. Based upon the design criteria of QoS, we seek to minimize the worst-case transmit power at MIMO

relay while guaranteeing the worst-case received SNR above a prescribed threshold at both sources. The formulation turns out nonconvex, but has been transformed into a convex optimization problem that can be efficiently solved by means of SDR and randomization technique. The robust approach has been compared with the nonrobust strategy [17], and the improved robustness of our proposed design has been verified in the simulations. Finally, we have investigated the feasibility issue of the proposed robust method.

Chapter 4

Conclusion and Future Work

4.1 Conclusions

In this thesis, we have addressed the impact of channel estimation error on the performance of AF two-way relaying. We have considered a system of two single-antenna sources communicating with each other with the assistance of either multiple single-antenna relays or a single MIMO relay station. The performance degradation and enhancement due to the estimation error for both cases have been investigated in Chapter 2 and 3, respectively.

In Chapter 2, when exploiting multiple single-antenna relays, we have derived the effective SNR subject to noisy channel estimation, and based on this, the system outage probability is given. In addition, we have derived the closed-form expression of the average system BER as well as the asymptotic expressions for both outage probability and BER. Furthermore, instead of employing all relays, we have examined the impact of imperfect CSI on the *Max-Min* RS scheme. To enhance the system performance to combat the negative impact of imperfect CSI, adaptive PA algorithm by minimizing either the outage probability or the average BER has been proposed. The adaptive PA has been suitably casted as GP problem, and solved efficiently by convex programming technique. We have validated the correctness of the derived expressions by means of numerical simulations and showed that adaptive PA scheme outperforms equal PA scheme under the aggregated effect of imperfect CSI.

Motivated by the advantages of MIMO systems, we have accommodated multiple antennas at the relay node. So in Chapter 3, a robust MIMO relay design strategy has been proposed for AF ANC-baed TWRN. The estimation error in CSI has been

explicitly taken into account, obtaining a robust solution less sensitive to this error. In particular, the worst-case philosophy has been utilized to achieve robustness. This approach strives to minimize the worst-case transmit power at the MIMO relay while guaranteeing the worst-case SNR above a prescribed threshold value at each source. The mathematical optimization problem corresponding to the robust MIMO relay design has been showed nonconvex. We have reformulated the design problem, and exploited the algorithm called two-stage SDR-based approximation consisting of relaxation and a combined randomization/scaling loop, to attain an approximated optimal solution to the original design. We have further compared the proposed MIMO relay with the nonrobust method by means of numerical simulations, and therefore verified its robustness against the channel uncertainty.

4.2 Future Work

In this thesis, we considered the distributed and centralized relaying to assist the information exchange between two single-antenna sources. There are several extensions on the system configuration which can be investigated as possible future work. For distributed relaying case, we may be able to extend our work to multiuser scenario, and introduce opportunistic relaying to the sources. For centralized relaying, we can first extend our single MIMO relay case to any configurations of relays or antennas. Moreover, we can also incorporate multiple antennas at both sources, and jointly design both the source and relay precoders.

Appendix A

Joint PDF of $\gamma_{A,i}^{\text{eff}}$ and $\gamma_{B,i}^{\text{eff}}$

In this appendix, the derivation of the joint PDF $Pr\left\{\gamma_{A,i}^{\text{eff}} < \gamma_{th}^{RS}, \gamma_{B,i}^{\text{eff}} < \gamma_{th}^{RS}\right\}$ is presented in detail.

First, by observing the relationship between $\gamma_{1,i}^{\text{eff}}$ and $\gamma_{4,i}^{\text{eff}}$, and $\gamma_{2,i}^{\text{eff}}$ and $\gamma_{3,i}^{\text{eff}}$, $\gamma_{A,i}^{\text{eff}}$ and $\gamma_{B,i}^{\text{eff}}$ are given by

$$\gamma_{A,i}^{\text{eff}} = \frac{\gamma_{1,i}^{\text{eff}}\gamma_{2,i}^{\text{eff}}}{\gamma_{1,i}^{\text{eff}} + \gamma_{2,i}^{\text{eff}}}, \text{ and } \gamma_{B,i}^{\text{eff}} = \frac{C_{1,i}C_{2,i}\gamma_{1,i}^{\text{eff}}\gamma_{2,i}^{\text{eff}}}{C_{1,i}\gamma_{1,i}^{\text{eff}} + C_{2,i}\gamma_{2,i}^{\text{eff}}}, \tag{A.1}$$

where

$$\begin{aligned} C_{1,i} &= \frac{\left(1 + \frac{P_B\sigma_{e_{g_i}}^2}{N_{r_i}} + \frac{P_A}{P_{r_i}}\frac{N_{A,i}}{N_{r_i}} + \frac{4P_A\sigma_{e_{h_i}}^2}{N_{r_i}}\right)\frac{P_{r_i}}{N_{B,i}}}{\left(1 + \frac{P_{r_i}\sigma_{e_{g_i}}^2}{N_{B,i}}\right)\frac{P_B}{N_{r_i}}}, \\ \text{and } C_{2,i} &= \frac{\left(1 + \frac{P_{r_i}\sigma_{e_{h_i}}^2}{N_{A,i}}\right)\frac{P_A}{N_{r_i}}}{\left(1 + \frac{P_B\sigma_{e_{h_i}}^2}{N_{r_i}} + \frac{P_B}{P_{r_i}}\frac{N_{B,i}}{N_{r_i}} + \frac{4P_B\sigma_{e_{g_i}}^2}{N_{r_i}}\right)\frac{P_{r_i}}{N_{A,i}}}, \end{aligned} \tag{A.2}$$

and $\gamma_{1,i}^{\text{eff}}$ and $\gamma_{2,i}^{\text{eff}}$ are independent exponentially distributed r.v.'s with mean given by (2.16).

Note that $\gamma_{A,i}^{\text{eff}}$ is symmetric in terms of $\gamma_{1,i}^{\text{eff}}$ and $\gamma_{2,i}^{\text{eff}}$, and $\gamma_{B,i}^{\text{eff}}$ is symmetric in terms of $C_{1,i}\gamma_{1,i}^{\text{eff}}$ and $C_{2,i}\gamma_{2,i}^{\text{eff}}$. Without loss of generality, we assume $C_{1,i} > C_{2,i}$. The scenario $C_{1,i} < C_{2,i}$ can be obtained similarly. By using the similar approach in [29], the inequality of $\frac{XY}{X+Y} < \min\{X, Y\}$ can be adopted to derive $\Pr\{\gamma_{A,i}^{\text{eff}} < \gamma_{th}^{RS}, \gamma_{B,i}^{\text{eff}} < \gamma_{th}^{RS}\}$, and a strict lower bound of system outage probability is equivalently

obtained. By utilizing the independence of $\gamma_{1,i}^{\text{eff}}$ and $\gamma_{2,i}^{\text{eff}}$ and the law of total probability, $\Pr\{\gamma_{A,i}^{\text{eff}} < \gamma_{th}^{RS}, \gamma_{B,i}^{\text{eff}} < \gamma_{th}^{RS}\}$ can be derived as

$$\begin{aligned}
&\Pr\{\gamma_{A,i}^{\text{eff}} < \gamma_{th}^{RS}, \gamma_{B,i}^{\text{eff}} < \gamma_{th}^{RS}\} \\
\leq &\Pr\{\min\{\gamma_{1,i}^{\text{eff}}, \gamma_{2,i}^{\text{eff}}\} < \gamma_{th}, \min\{C_{1,i}\gamma_{1,i}^{\text{eff}}, C_{2,i}\gamma_{2,i}^{\text{eff}}\} < \gamma_{th}^{RS}\}, \\
= &\Pr\{\gamma_{1,i}^{\text{eff}} > \gamma_{2,i}^{\text{eff}}\} \Pr\{\gamma_{2,i}^{\text{eff}} < \gamma_{th}^{RS}, \gamma_{2,i}^{\text{eff}} < \frac{\gamma_{th}^{RS}}{C_{2,i}}\} \\
&+ \Pr\{\frac{C_{2,i}}{C_{1,i}}\gamma_{2,i}^{\text{eff}} < \gamma_{1,i}^{\text{eff}} < \gamma_{2,i}^{\text{eff}}\} \Pr\{\gamma_{1,i}^{\text{eff}} < \gamma_{th}^{RS}, \gamma_{2,i}^{\text{eff}} < \frac{\gamma_{th}^{RS}}{C_{2,i}}\} \\
&+ \Pr\{\gamma_{1,i}^{\text{eff}} < \frac{C_{2,i}}{C_{1,i}}\gamma_{2,i}^{\text{eff}}\} \Pr\{\gamma_{1,i}^{\text{eff}} < \gamma_{th}^{RS}, \gamma_{1,i}^{\text{eff}} < \frac{\gamma_{th}^{RS}}{C_{1,i}}\}.
\end{aligned} \tag{A.3}$$

Since $\gamma_{1,i}^{\text{eff}}$ and $\gamma_{2,i}^{\text{eff}}$ are independent exponentially distributed r.v.'s with parameters denoted by $\lambda_{1,i}$ and $\lambda_{2,i}$, respectively, we can determine each term in (A.3) and obtain

$$\begin{aligned}
&\Pr\{\gamma_{A,i}^{\text{eff}} < \gamma_{th}^{RS}, \gamma_{B,i}^{\text{eff}} < \gamma_{th}^{RS}\} \\
\leq &\frac{\lambda_{2,i}}{\lambda_{1,i}+\lambda_{2,i}}\left(1 - e^{-\lambda_{2,i}\min\{\gamma_{th}^{RS}, \gamma_{th}^{RS}/C_{2,i}\}}\right) \\
&+ \left(\frac{\lambda_{1,i}}{\lambda_{1,i}+\lambda_{2,i}} - \frac{\lambda_{1,i}}{\lambda_{1,i}+\frac{C_{1,i}}{C_{2,i}}\lambda_{2,i}}\right)\left(1 - e^{-\lambda_{1,i}\gamma_{th}^{RS}}\right)\left(1 - e^{-\lambda_{2,i}\gamma_{th}^{RS}/C_{2,i}}\right) \\
&+ \frac{\lambda_{1,i}}{\lambda_{1,i}+\frac{C_{1,i}}{C_{2,i}}\lambda_{2,i}}\left(1 - e^{-\lambda_{1,i}\min\{\gamma_{th}^{RS}, \gamma_{th}^{RS}/C_{1,i}\}}\right).
\end{aligned} \tag{A.4}$$

The authors in [29] has shown that irrespective of the values of channel variances, the lower bound of the system outage probability based on the upper bound in (A.4) is very close to the exact outage in the whole SNR range.

Bibliography

[1] J.N. Laneman and G.W. Wornell, "Distributed space-time-coded protocols for exploiting cooperative diversity in wireless networks," *IEEE Trans. Inf. Theory*, vol. 49, pp. 2415–2425, Oct. 2003.

[2] J.N. Laneman, D.N.C. Tse and G.W. Wornell, "Cooperative diversity in wireless networks: efficient protocols and outage behavior," *IEEE Trans. Inf. Theory*, vol. 50, pp. 3062–3080, Dec. 2004.

[3] A. Nosratinia, T.E. Hunter and A. Hedayat, "Cooperative communication in wireless networks," *IEEE Commun. Mag.*, vol. 42, pp. 74–80, Oct. 2004.

[4] C. Shannon, "Two-way communication channels," in *Proc. 4th Berkeley Symp. Math. Stat. Prob.*, vol. 1, pp. 611–644, Univ. California Press, 1961.

[5] B. Rankov and A. Wittneben, "Spectral efficient protocols for half-duplex fading relay channels," *IEEE J. Sel. Areas Commun.*, vol. 25, pp. 379–389, Feb. 2007.

[6] F. Gao, C. Schnurr, I. Bjelakovic and H. Boche, "Optimal channel estimation and training design for two-way relay networks," *IEEE Trans. Commun.*, vol. 57, pp. 3024–3033, Oct. 2009.

[7] S. Katti, S. Gollakota, and D. Katabi, "Embracing wireless interference: analog network coding," *SIGCOMM Comput. Commun. Rev.*, vol. 37, pp. 397–408, August 2007.

[8] S. J. Kim, P. Mitran, and V. Tarokh, "Performance bounds for bidirectional coded cooperation protocols," *IEEE Trans. Inf. Theory*, vol. 54, pp. 5235 –5241, Nov. 2008.

[9] Y. Zhang, Y. Ma, and R. Tafazolli, "Power allocation for bidirectional af relaying over raleigh fading channels," *IEEE Commun. Lett.*, vol. 14, pp. 145–147, Feb. 2010.

[10] X. J. Zhang and Y. Gong, "Adaptive power allocation in two-way amplify-and-forward relay networks," in *Proc. of IEEE Int. Conf. on Commun. (ICC)*, June 2009.

[11] Ha X. Nguyen, Ha N. Nguyen and Tho Le-Ngoc, "Diversity analysis of relay selection schemes for two-way wireless relay networks," *Wireless Personal Communications*, Jan. 2010.

[12] L. Song, "Relay selection for two-way relaying with amplify-and-forward protocols," *IEEE Trans. Veh. Technol.*, vol. 60, pp. 1954–1959, May 2011.

[13] T.H. Pham, Y.C. Liang, A.Nallanathan and G.H. Krishna, "On the design of optimal training sequence for bi-directional relay networks," *IEEE Signal Process. Lett.*, vol. 16, pp. 200–203, Mar. 2009.

[14] R. Annavajjala, "On optimum regenerative relaying with imperfect channel knowledge," *IEEE Trans. Signal Process.*, vol. 58, pp. 1928–1934, Mar. 2010.

[15] S.S. Ikki, O. Amin and M. Uysal, "Performance analysis of cooperative diversity networks with imperfect channel estimation," in *Proc. of IEEE Int. Conf. on Commun. (ICC)*, pp. 1–5, May 2010.

[16] S. Han, S. Ahn, E. Oh and D. Hong, "Effect of channel-estimation error on BER performance in cooperative transmission," *IEEE Trans. Veh. Technol.*, vol. 58, pp. 2083–2088, May 2009.

[17] R. Zhang, Y.-C. Liang, C. C. Chai, and S. Cui, "Optimal beamforming for two-way multi-antenna relay channel with analogue network coding," *IEEE J. Sel. Areas Commun.*, vol. 27, pp. 699–712, Jun. 2009.

[18] C. Li, L. Yang, and W.-P. Zhu, "Two-Way MIMO Relay Precoder Design with Channel State Information," *IEEE Trans. Commun.*, vol. 58, pp. 3358–3363, Dec. 2010.

[19] K.-J. Lee, H. Sung, E. Park, and I. Lee, "Joint Optimization for One and Two-Way MIMO AF Multiple-Relay Systems," *IEEE Trans. Wireless Commun.*, vol. 9, pp. 3671–3681, Dec. 2010.

[20] M. Bengtsson, *Optimal and suboptimal transmit beamforming.* Handbook of Antennas in Wireless Communications, 2001.

[21] B. Chalise and L. Vandendorpe, "MIMO Relay Design for Multipoint-to-Multipoint Communications With Imperfect Channel State Information," *IEEE Trans. Signal Process.*, vol. 57, pp. 2785–2796, Jul. 2009.

[22] B. Chalise, "Optimization of MIMO relays for multipoint-to-multipoint communications: nonrobust and robust designs," *IEEE Trans. Signal Process.*, vol. 58, pp. 6355 –6368, Dec. 2010.

[23] P. Ubaidulla and A. Chockalingam, "Relay Precoder Optimization in MIMO-Relay Networks with Imperfect CSI." Accepted for publication in a future issue of *IEEE Trans. Signal Process.*, 2011.

[24] S. Boyd, S.-J. Kim, L. Vandenberghe, and A. Hassibi, "A tutorial on geometric programming," *Optimization and Engineering*, vol. 8, pp. 67–127, 2007.

[25] M. Chiang, C. W. Tan, D. Palomar, D. O'Neill, and D. Julian, "Power control by geometric programming," *IEEE Trans. Wireless Commun.*, vol. 6, pp. 2640–2651, Jul. 2007.

[26] M. Chiang, "Geometric programming for communication systems.," *Foundations and Trends in Communications and Information Theory*, pp. 1–156, 2005.

[27] M. Grant and S. Boyd, "CVX: Matlab software for disciplined convex programming, version 1.21." `http://cvxr.com/cvx`, Apr. 2011.

[28] S. Roy and P. Fortier, "Maximal-ratio combining architectures and performance with channel estimation based on a training sequence," *IEEE Trans. Wireless Commun.*, vol. 3, pp. 1154–1164, Jul. 2004.

[29] Z. Yi, M. Ju, and I.-M. Kim, "Outage probability and optimum power allocation for analog network coding," *IEEE Trans. Wireless Commun.*, vol. 10, pp. 407–412, Feb. 2011.

[30] M. Hasna and M.-S. Alouini, "End-to-end performance of transmission systems with relays over rayleigh-fading channels," *IEEE Trans. Wireless Commun.*, vol. 2, pp. 1126–1131, Nov. 2003.

[31] M. Abramowitz and I. A. Stegun, *Handbook of Mathematical Functions with Formulas, Graphs, and Mathematical Tables*. New York: Dover, 1970.

[32] K. G. Seddik, A. K. Sadek, W. Su and K. J. R. Liu, "Outage analysis and optimal power allocation for multimode relay networks," *IEEE Signal Process. Lett.*, vol. 14, pp. 377–380, May 2007.

[33] S.V. Amari and R.B. Misra, "Closed-form expressions for distribution of sum of exponential random variables," *IEEE Trans. Rel.*, vol. 46, pp. 519–522, Dec. 1997.

[34] A. Ribeiro, X. Cai and G. B. Giannakis, "Symbol error probabilities for general Cooperative links," *IEEE Trans. Wireless Commun.*, vol. 4, pp. 1264–1273, May 2005.

[35] M. Simon and M. Alouini, *Digital communication over fading channels: a unified approach to performance analysis*. New York: John Wiley & Sons, 2000.

[36] W. Su, A. Sadek and K. Ray Liu, "Cooperative communication protocols in wireless networks: performance analysis and optimum power allocation," *Wireless Personal Communications*, vol. 44, pp. 181–217, Jan. 2008.

[37] Y. Jing, "A relay selection scheme for two-way amplify-and-forward relay networks," in *Int. Conf. on Wireless Commun. Signal Process. (WCSP)*, pp. 1–5, Nov. 2009.

[38] A. Goldsmith, *Wireless Communications*. New York, NY, USA: Cambridge University Press, 2005.

[39] Y. Zhao, R. Adve and T. J. Lim, "Symbol error rate of selection amplify-and-forward relay systems," *IEEE Commun. Lett.*, vol. 10, pp. 757–759, Nov. 2006.

[40] I. S. Gradshteyn and I. M. Ryzhik, *Table of Integrals, Series, and Products, seventh edition*. Academic Press, 2007.

[41] S. Boyd and L. Vandenberghe, *Convex Optimization*. Cambridge University Press, Mar. 2004.

[42] M. Botros and T. Davidson, "Convex Conic Formulations of Robust Downlink Precoder Designs With Quality of Service Constraints," *IEEE J. Sel. Topics Signal Process.*, vol. 1, pp. 714–724, Dec. 2007.

[43] M. Payaro, A. Pascual-Iserte, and M. Lagunas, "Robust Power Allocation Designs for Multiuser and Multi-antenna Downlink Communication Systems through Convex Optimization," *IEEE J. Sel. Areas Commun.*, vol. 25, pp. 1390–1401, Sept. 2007.

[44] A. Pascual-Iserte, D. Palomar, A. Perez-Neira, and M. Lagunas, "A robust maximin approach for MIMO communications with imperfect channel state information based on convex optimization," *IEEE Trans. Signal Process.*, vol. 54, pp. 346–360, Dec. 2006.

[45] G. Zheng, K.-K. Wong, and T.-S. Ng, "Robust Linear MIMO in the Downlink: A Worst-Case Optimization with Ellipsoidal Uncertainty Regions," *EURASIP Journal on Advances in Signal Processing*, vol. 2008, pp. 1–16, 2008.

[46] E. Karipidis, N. Sidiropoulos, and Z.-Q. Luo, "Quality of Service and Max-Min Fair Transmit Beamforming to Multiple Cochannel Multicast Groups," *IEEE Trans. Signal Process.*, vol. 56, pp. 1268–1279, Mar. 2008.

[47] N. D. Sidiropoulos, T. Davidson, and Z.-Q. Luo, "Transmit beamforming for physical-layer multicasting," *IEEE Trans. Signal Process.*, vol. 54, pp. 2239–2251, June 2006.

[48] E. Matskani, N. Sidiropoulos, Z. quan Luo, and L. Tassiulas, "Convex approximation techniques for joint multiuser downlink beamforming and admission control," *IEEE Trans. Wireless Commun.*, vol. 7, pp. 2682 –2693, July 2008.

[49] Wikipedia, "Chi-square distribution – *Wikipedia, The Free Encyclopedia*."

[50] M. Biguesh, S. Shahbazpanahi, and A. B. Gershman, "Robust downlink power control in wireless cellular systems," *EURASIP J. Wirel. Commun. Netw.*, vol. 2004, pp. 261–272, December 2004.

[51] J. Lofberg, "Yalmip: a toolbox for modeling and optimization in matlab," in *Proc. CACSD Conf.*, (Taipei, Taiwan), Sept. 2004.

[52] J. Löfberg, "Automatic robust convex programming," *Optimization Methods and Software*, 2010.

[53] Z.-Q. Luo and W. Yu, "An introduction to convex optimization for communications and signal processing," *IEEE J. Sel. Areas Commun.*, vol. 24, pp. 1426–1438, Aug. 2006.